

を障害された(酵素を持たない)細胞が取り込むことで蓄積された異常な物質が低下するためと考えられている。MSCをlysosome病の治療に用いる場合には、①移植したMSCが損傷した組織で正常な細胞に分化する、②移植したMSCから分化した細胞が欠損している酵素を分泌する2つの機序が考えられる。Huler症候群は、 α -L-iduronidaseの欠損のため、heparan sulfateとdermatan sulfateがlysosomeに蓄積し、肝脾腫、心疾患、骨格異常、水頭症や精神遅滞を来す疾患である。異染色性白質ジストロフィー (metachromatic leukodystrophy: MLD) は、arylsulfatase A欠損のため sulfatidesの蓄積し、中枢神経と末梢神経の脱髄のため歩行困難、四肢麻痺や精神遅滞を引き起こす。Kocらは²⁾、以前骨髄移植を受けた5人のHuler症候群と6人のMLDに、同一ドナーの骨髄細胞から得られたMSCを、体重当たり 2.0×10^6 から 10.0×10^6 細胞を投与し臨床効果を検討した。副作用は認められなかった。MSC投与後の骨髄細胞のキメリズム検査では、day 60の時点で、2例に0.4%と2.0%のドナー由来のMSCが確認された。骨密度の改善は軽度であったが、4人のMLDで神経伝達速度の改善を認めた(図1)。残念ながら、精神や身体の発達には変化を認めなかった。骨形成不全症は、骨形成の主要な蛋白であるI型collagenが形成されないため生じる疾患で、多発性の骨折を来しやすく四肢の変形や短身長を生じる。Horwitzらは³⁾、骨髄移植を受けた6人の小児に、同一のドナーの骨髄細胞からMSCを分離し増殖させた後、neomycin耐性遺伝子を組み込んだretrovirusをMSCにtransfectionした。骨髄移植後18~34カ月を経過した6人の子どもに、遺伝子マーキングしたMSCを体

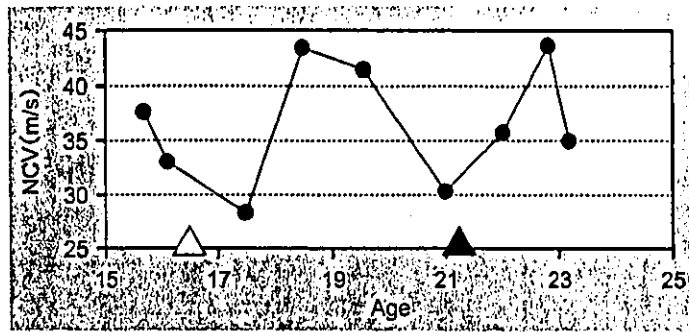


図1 MSC投与後の神経伝達速度の変化

MLDの患者に骨髄移植(△)を行ったところ、peroneal nerveの神経伝達速度は改善したが、移植約4年後低下した。同一ドナーからのMSCを投与(▲)したところ、神経伝達速度は再び改善した。

(文献2より引用)

重当たり 1.0×10^6 から 5.0×10^6 細胞を投与した。重篤な副作用は認められず、5人では骨、皮膚や骨髄stromaに移植したMSCの存在が確認された。臨床効果は明らかで、MSCの生着が確認された5人では、MSCの移植6カ月後の成長速度は、同年齢の子どもの60~94%に回復した(図2)。MSCは、lysosome病や骨形成不全症に有効である可能性が示された。

2. 造血幹細胞移植時の生着促進を目的としたMSCの投与

MSCは骨髄微小環境を構成し、造血幹細胞の支持能を有するので、造血幹細胞移植時にMSCを同時投与すると、移植した造血幹細胞の生着と造血回復を促進する効果が期待される。Kocらは⁴⁾、32人の乳癌の患者の骨髄細胞からMSCを分離し増殖した。28人の患者で、自家末梢血幹細胞移植後の1または24時間後に体重当たり 1×10^6 細胞以上の自家MSCを投与した。MSC投与に関連した副作用は認められなかった。移植後の造血の回復は速やかで、好中球が $500/\mu\text{L}$ を超え

(略語一覧)

MLD (metachromatic leukodystrophy; 異染色性白質ジストロフィー)

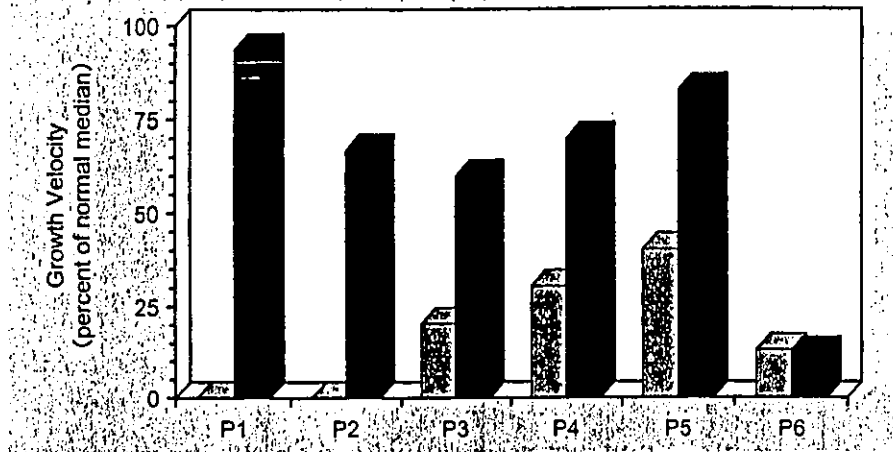


図2 MSC投与後の身長伸びの速度

骨形成不全症に対して骨髄移植を行い、その後、同一ドナーからMSCを投与した。MSCの投与前(灰色)とMSCの投与6カ月後(黒)に、身長伸びを比較したところ、投与後にMSCの存在が確認された5人(P1～P5)では、身長伸びの速度は増加した。(文献3より引用)

る日は移植後8日、血小板が2万/ μ Lを超える日は移植後8.5日であった。

近年、臍帯血移植は盛んに行われ、本邦における非血縁者造血幹細胞移植の約半分を占めるようになった。臍帯移植で問題となるのは、移植細胞数の少なさが原因と考えられる生着遅延や拒絶である。複数の臍帯血を同時に移植する試みが行われているが、複数の臍帯血を同時移植することによって、移植細胞数を増加しても、移植後の血球の著明な回復促進は生じないこと、原因として生着後どちらか一方の臍帯血由来の造血が優位となることが報告されている¹⁾。最近、Kimらは²⁾2種類のヒト組織適合抗原(human leukocyte antigen: HLA)が3～6座不一致の臍帯血を、CD34陽性細胞数を同数含む単核細胞に調整後、第3者から得られたMSCと一緒にnon-obese diabetic/severe combined immunodeficient (NOD/SCID) マウスに移植し、short tandem repeat

マーカによる移植後のキメリズムの割合を検討した。MSCを同時に移植すると、2種類の造血がほぼ等しく起ること(表1)、ヒト由来のCD71(transferrin receptor)陽性の増殖細胞が約2倍に増加すること(図3)を報告した。このMSCの作用は、2つの臍帯血中に含まれるリンパ球のgraft-versus-graft reactionを抑制することによって、各々の造血幹細胞の生着が促されたと考えられた。

3. GVHD 予防または治療を目的とした MSC の投与

MSCは、mitogen 刺激やmixed lymphocyte reactionによるT細胞の活性化を強く抑制することが知られている³⁾。最近、MSCは成熟した樹状細胞(DC1)に作用し腫瘍壊死因子(tumor necrosis factor: TNF) α の産生を抑制すること、成熟

【略語一覧】

HLA (human leukocyte antigen; ヒト組織適合抗原)

NOD/SCID (non-obese diabetic/severe combined immunodeficient)

DC (dendritic cells; 樹状細胞)

表1 2種類の臍帯血同時移植後のキメリズム

| 臍帯血移植 | 移植したマウス(数) | ドナーA(%) | ドナーB(%) | A:B |
|-------------|------------|------------|------------|-------|
| A+B | 26 | 73.5 ± 3.1 | 26.5 ± 3.1 | 2.8:1 |
| (A+B) + MSC | 19 | 64.5 ± 2.7 | 35.5 ± 2.7 | 1.8:1 |

NOD/SCID マウスに、同数の CD34 陽性細胞を含む A と B の 2 種類の臍帯血を同時移植し、移植後のヒト細胞のキメリズムを検査した。A と B を同時移植すると、どちらか一方の臍帯血(表の場合には A)の造血が優位となるが、MSC を同時投与すると、A と B の造血がほぼ等しくなる。(文献 6 より引用)

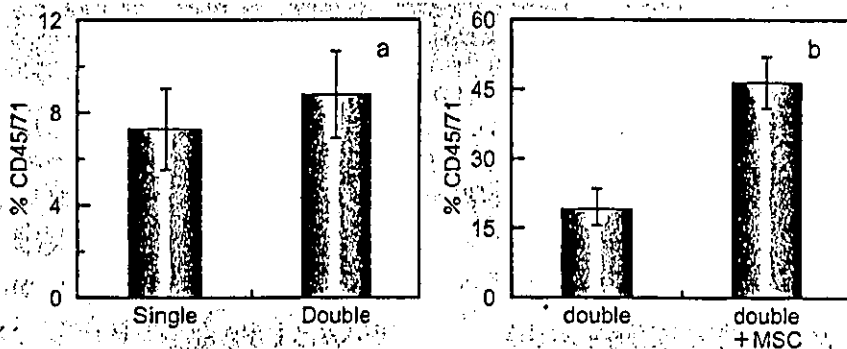


図3 臍帯血移植の生着に及ぼす MSC の効果

同数の CD34 陽性細胞数を含む臍帯血単核細胞 2 種類を、NOD/SCID に同時移植 (double) した。臍帯血のみの移植 (double) では移植 CD34 陽性細胞数を 2 倍にしても、移植後の生着細胞の増加は認められなかった (a) が、MSC を一緒に移植すると (double + MSC)、生着する細胞数は約 2 倍に増加した (b)。(文献 6 より引用)

した樹状細胞 (DC2) に作用し interleukin (IL)-10 の産生を増加させることによって、Th1 細胞からの IFN γ 産生を抑制し Th2 細胞からの IL-4 産生を誘導することが示された (図 4)⁹⁾。また、MSC は regulatory T 細胞を増加させ、natural killer (NK) 細胞からの IFN γ 産生を抑制した (図 4)。また、MSC 自身の抗原性は低いことが報告されている。このような MSC による免疫修飾作用は、GVHD の予防や治療に有効である可能性がある。

米国のベンチャー企業の Osiris は、第 3 者の骨髄細胞から得られた MSC を、HLA 一致ドナーから

の骨髄移植時に同時投与し、GVHD 発症率、移植関連死亡 (transplant related mortality: TRM)、生存率を比較する臨床試験を行った (図 5)。MSC を投与した群では、慢性 GVHD の頻度の低下、TRM の低下、生存率と無病生存率の増加が認められた。MSC 投与による重篤な副作用は認められず、MSC は同種造血幹細胞移植後の GVHD 予防に有用と考えられた。本邦においても、HLA 一致ドナーからの骨髄移植時に、GVHD 予防を目的として非血縁者 MSC を同時投与する第 1 相臨床試験が計画されている。最近、

《略語一覧》

TNF (tumor necrosis factor; 腫瘍壊死因子)
NK (natural killer)

IL (interleukin)
TRM (transplant related mortality; 移植関連死亡)

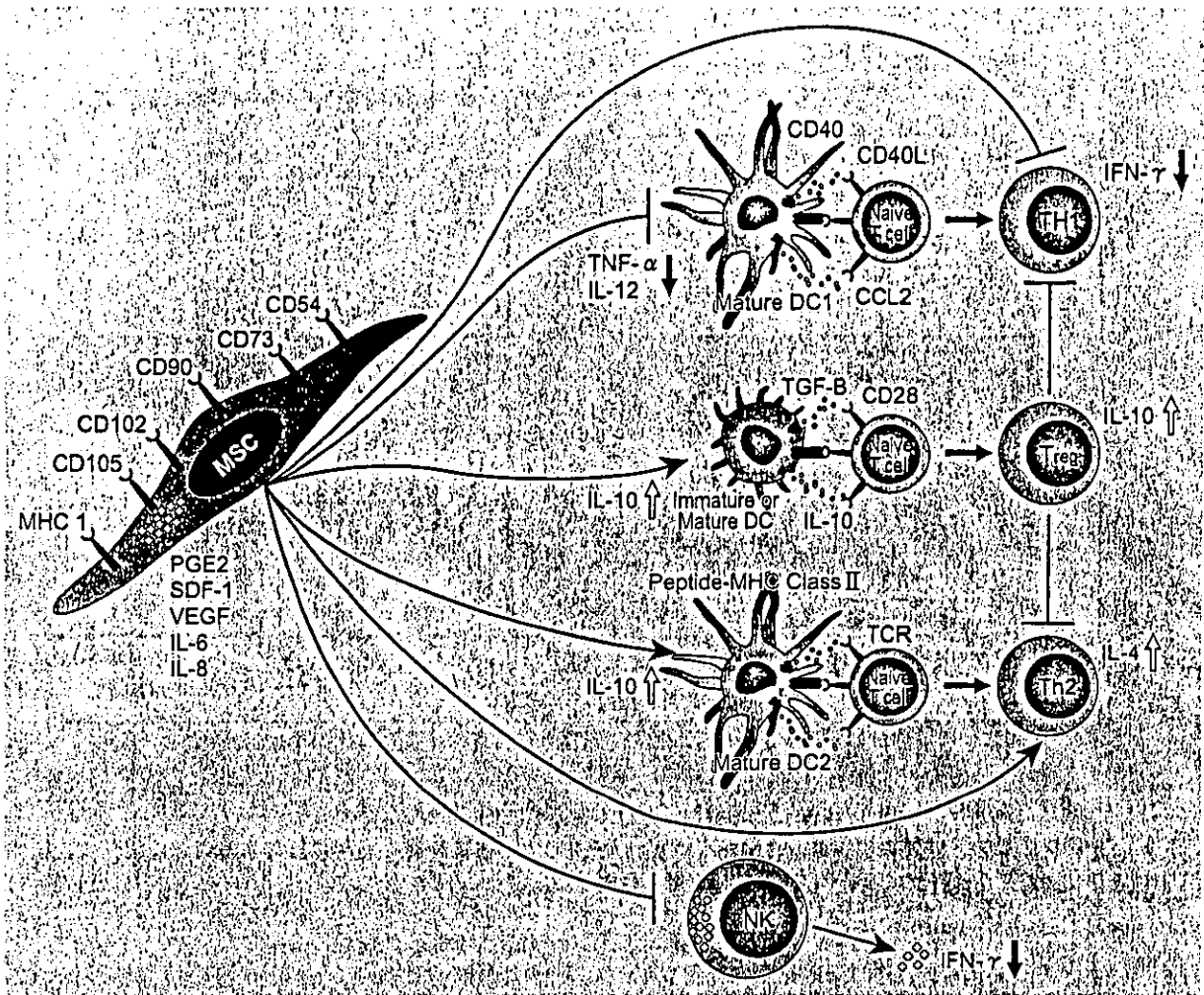


図4 MSCの免疫調節作用

MSCは、樹状細胞のTNF α の分泌を抑制し、IL-10の分泌を促進することによって、樹状細胞の成熟と機能に影響を及ぼし、その結果として抗炎症作用と免疫寛容をもたらすと考えられる。

死亡 (transplant related mortality : TRM)

(文献8より引用)

興味ある症例報告がなされた(図6)⁹⁾。症例は9歳の急性リンパ性白血病(acute lymphocytic leukemia : ALL) 男児で、第3寛解期にHLA一致の非血縁女性ドナーから、同種末梢血幹細胞移植を受けた。移植後、急性GVHD(皮疹、下痢と腹痛、黄疸)が出現した。各種治療 (psoralen with ultraviolet-A light (PUVA), methypredniso-

lone, inflixmab, daclizmab, mycophenolate mofetil, methotrexate)を試みたにも係らずIV度の急性GVHDに進展した。そこで、児の母親の骨髄からMSC分離し増殖させ、体重当たり 2×10^6 個のMSCを投与した。投与後、速やかな血清ビリルビンの低下と下痢の減少が認められた。その後、骨髄で微小残存白血病を認めたため、移植片

《略語一覧》

ALL (acute lymphocytic leukemia ; 急性リンパ性白血病)

PUVA (psoralen with ultraviolet-A light)

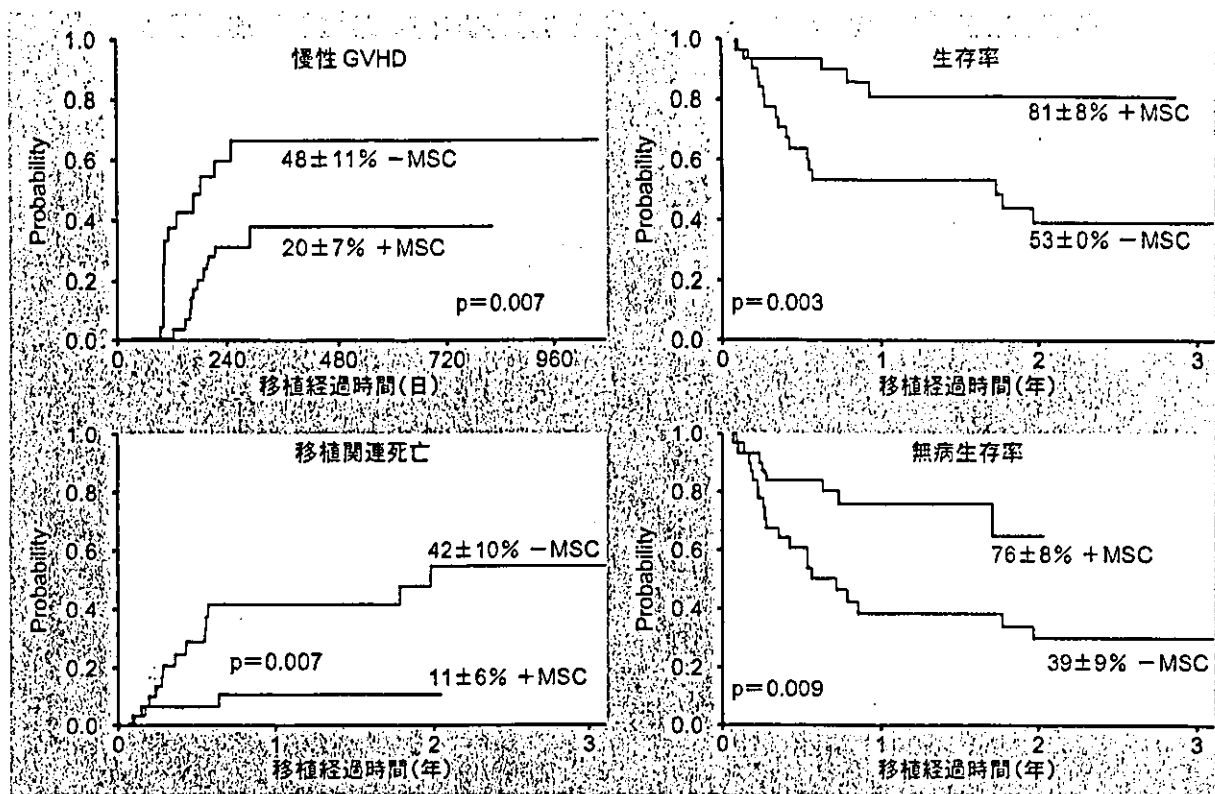


図5 GVHD, 移植関連死亡, 生存率に及ぼす MSC の効果

ドナーとレシピエント以外の第3者の骨髄から得られたMSCを、移植骨髄と同時に投与することによって、慢性GVHDと移植関連死亡は有意に低下し、生存率は有意に増加した。(Osiris 資料)

対白血病効果 (graft-versus-leukemia effect : GVL effect)を誘導する目的で cyclosporin を減量したところ、再度 GVHD が出現した。そこで、体重当たり 1×10^6 個の母親の MSC を再度投与したところ GVHD は終息した。MSC の投与に伴う副作用を認めなかった。著者らの施設では、IV 度の急性 GVHD が出現した 25 人中で MSC を投与した本例のみが、唯一の生存例であった。

おわりに

MSC を用いた同種免疫の制御は、現在日常の臨床で行われている薬物を用いたそれに匹敵する

効果が期待される。MSC 自身の抗原性が低いことから第3者(非自己および非ドナー)の MSC を用いることが出来ること、MSC 投与に伴う重篤な副作用が報告されていないことは、MSC を臨床応用するに当り大きな利点と思われる。MSC は多分化能を有するため、異所性の分化が生じる可能性は否定できないが、現在までに行われた臨床試験でそのような報告はない。今後、本邦においても造血幹細胞移植時の生着促進、GVHD 予防や GVHD 治療に対して、MSC の有用性を検討する臨床試験が早期に実施されることが期待されている。

【略語一覧】

GVL effect (graft-versus-leukemia effect ; 移植片対白血病効果)

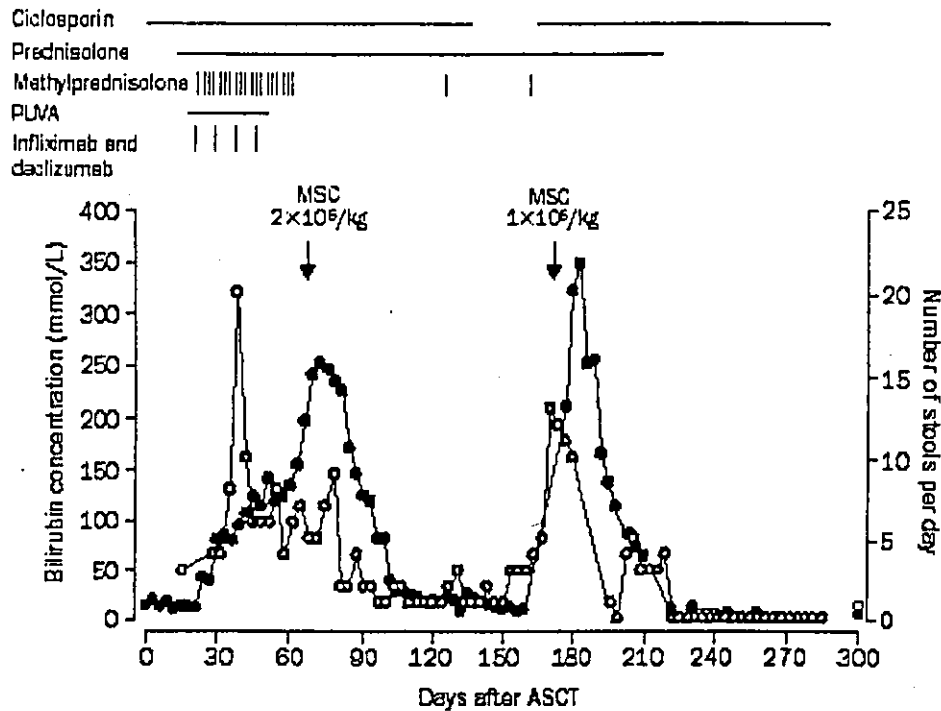


図6 臨床経過

難治性の肝と腸のGVHDに、母親(非ドナー)の骨髓から得られたMSCを2回投与したところ、血清ビリルビン(●)と便の回数(○)は著明に低下した。(文献9より引用)

文献

- 1) Pittenger MF, Martin BJ : Mesenchymal stem cells and their potential as cardiac therapeutics. *Circ Res* 95 : 9-20, 2004
- 2) Koc ON, et al : Allogeneic mesenchymal stem cell infusion for treatment of metachromatic leukodystrophy (MLD) and Hurler syndrome (MPS-IH) . *Bone Marrow Transplant* 30 : 215-222, 2002
- 3) Horwitz EM, et al : Isolated allogeneic bone marrow-derived mesenchymal cells engraft and stimulate growth in children with osteogenesis imperfecta : Implications for cell therapy of bone. *Proc Natl Acad Sci U S A* 99 : 8932-8937, 2002
- 4) Koc ON, et al : Rapid hematopoietic recovery after coinfusion of autologous-blood stem cells and culture-expanded marrow mesenchymal stem cells in advanced breast cancer patients receiving high-dose chemotherapy. *J Clin Oncol* 18 : 307-316, 2000
- 5) Barker JN, et al : Transplantation of two partially HLA-matched umbilical cord blood units to enhance engraftment in adults with hematologic malignancy. *Blood*, 2004, [Epub ahead of print]
- 6) Kim DW, et al : Cotransplantation of third-party mesenchymal stromal cells can alleviate single-donor predominance and increase engraftment from double cord transplantation. *Blood* 103 : 1941-1981, 2004
- 7) Maitra B, et al : Human mesenchymal stem cells support unrelated donor hematopoietic stem cells and suppress T-cell activation. *Bone Marrow Transplant* 33 : 597-604, 2004
- 8) Aggarwal S, Pittenger MF : Human mesenchymal stem cells modulate allogeneic immune cell responses. *Blood*, 2004 [Epub ahead of print] .
- 9) O' Donoghue K, et al : Microchimerism in female bone marrow and bone decades after fetal mesenchymal stem-cell trafficking in pregnancy. *Lancet* 364 : 179-182, 2004



AAV Vector-Mediated Microdystrophin Expression in a Relatively Small Percentage of *mdx* Myofibers Improved the *mdx* Phenotype

Madoka Yoshimura,^{1,2} Miki Sakamoto,¹ Madoka Ikemoto,¹ Yasushi Mochizuki,¹ Katsutoshi Yuasa,¹ Yuko Miyagoe-Suzuki,¹ and Shin'ichi Takeda^{1,*}

¹Department of Molecular Therapy, National Institute of Neuroscience, National Center of Neurology and Psychiatry, 4-1-1 Ogawa-higashi, Kodaira, Tokyo 187-8502, Japan

²Department of Neurology, Division of Neuroscience, Graduate School of Medicine, University of Tokyo, Hongo 7-3-1, Tokyo 113-8655, Japan

*To whom correspondence and reprint requests should be addressed. Fax: +81 42 346 1750. E-mail: takeda@ncnp.go.jp.

Available online 19 August 2004

Duchenne muscular dystrophy (DMD) is a lethal disorder of skeletal muscle caused by mutations in the *dystrophin* gene. Adeno-associated virus (AAV) vector-mediated gene therapy is a promising approach to the disease. Although a rod-truncated microdystrophin gene has been proven to ameliorate dystrophic phenotypes, the level of microdystrophin expression required for effective gene therapy by an AAV vector has not been determined yet. Here, we constructed a recombinant AAV type 2 vector, AAV2-MCK Δ CS1, expressing microdystrophin (Δ CS1) under the control of a muscle-specific MCK promoter and injected it into TA muscles of 10-day-old and 5-week-old *mdx* mice. AAV2-MCK Δ CS1-mediated gene transfer into 5-week-old *mdx* muscle resulted in extensive and long-term expression of microdystrophin and significantly improved force generation. Interestingly, 10-day-old injected muscle expressed microdystrophin in a limited number of myofibers but showed hypertrophy of microdystrophin-positive muscle fibers and considerable recovery of contractile force. Thus, we concluded that AAV2-MCK Δ CS1 could be a powerful tool for gene therapy of DMD.

Key Words: Duchenne muscular dystrophy, gene therapy, adeno-associated virus vector, dystrophin, microdystrophin, skeletal muscle, *mdx* mouse, hypertrophy

INTRODUCTION

Duchenne muscular dystrophy (DMD) is an X-linked, lethal disorder of skeletal muscle caused by mutations in the *dystrophin* gene. There is no effective treatment for the disease at present, although gene therapy could be an attractive approach to the disease.

Several methods of gene transfer have been tried for the treatment of dystrophin-deficient muscular dystrophy: naked plasmid injection [1], full-length dystrophin cDNA transfer via a gutted adenovirus vector [2,3], forced splicing using oligonucleotides [4], and gene repair by a chimeric RNA/DNA oligonucleotide [5]. Among several gene transfer methods, an adeno-associated virus (AAV) vector-mediated gene transfer is one of the most promising approaches to DMD because AAV vectors have been shown to evoke minimal immune responses and mediate long-term transgene expression in skeletal muscle [6–8]. Since the capacity

of an AAV vector to incorporate an exogenous gene is limited to 4.9 kb, several groups have attempted to truncate the 14-kb dystrophin cDNA to obtain functional microdystrophins to be inserted into AAV vectors [9–13]. We previously constructed three rod-truncated microdystrophins and generated transgenic *mdx* mice expressing these microdystrophins. Among the three microdystrophins tested, only the 4.9-kb microdystrophin CS1 completely prevented muscle degeneration of dystrophin-deficient *mdx* mice [14]. Based on this result, we generated an AAV vector carrying Δ CS1 microdystrophin cDNA, a modified version of CS1 cDNA, and injected the vectors (designated AAV2-MCK Δ CS1) directly into both 10-day-old and 5-week-old *mdx* muscles. In this study, we demonstrate that AAV vector-injected *mdx* muscles showed functional recovery even 24 weeks after treatment. Surprisingly, when introduced into neonatal muscle, microdystrophin expression in a relatively small percentage of



muscle fibers dramatically improved the contractile properties of dystrophic muscle. This improvement in contractile force was thought to be achieved by hyperphosphorylated microdystrophin-positive muscle fibers.

RESULTS

Construction of an AAV-2 Vector Carrying Microdystrophin Δ CS1

We constructed an AAV-2 vector encoding microdystrophin Δ CS1 under the control of a truncated, muscle-specific creatine kinase (MCK) promoter [15]. We designated this recombinant AAV vector AAV2-MCK Δ CS1. CS1, which has the N-terminal, actin-binding domain, four rod repeats and three hinges, the cysteine-rich domain, and the C-terminal domain, effectively rescued dystrophic phenotypes when introduced as a transgene [14]. To shorten CS1 cDNA (4.9 kb) further, we deleted the 5' and 3' untranslated regions (UTRs) and exons 71–78 (alternative splicing regions of dystrophin mRNA) by PCR techniques. We named the resultant 3.8-kb cDNA Δ CS1 (Fig. 1).

Expression of Δ CS1 Microdystrophin at the Sarcolemma after AAV2-MCK Δ CS1-Mediated Gene Transfer into *mdx* Muscle

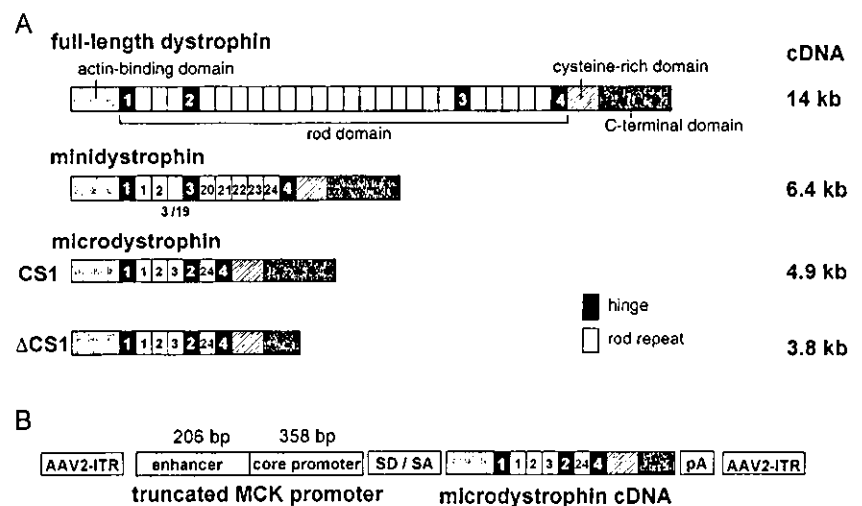
We injected AAV2-MCK Δ CS1 into tibialis anterior (TA) muscles of 10-day-old and 5-week-old dystrophin-deficient *mdx* mice (7.5×10^{10} vector genomes (vg) for neonatal muscle; 2.5×10^{11} vg for young muscle). In a natural course, 10-day-old *mdx* muscle shows no obvious dystrophic changes, while 5-week-old *mdx* muscle shows active cycles of the degeneration–regeneration process. We also analyzed contralateral TA muscles from the treated *mdx* mice and TA muscles from age-matched

C57BL/10 (B10) mice as controls. When examined at 8 and 24 weeks after AAV2-MCK Δ CS1 injection, Δ CS1 had correctly localized at the sarcolemma (Figs. 2A and 2C). Western blot using a dystrophin antibody showed a band of the expected size (138 kDa) in the AAV vector-injected *mdx* muscles (Fig. 2G). Most of the Δ CS1-positive fibers were peripherally nucleated when AAV2-MCK Δ CS1 was injected into 10-day-old *mdx* muscles (Figs. 2A and 2B). In contrast, we observed both centrally and peripherally nucleated fibers when the vectors were injected into 5-week-old *mdx* muscle (Figs. 2C and 2D). The mean percentages of Δ CS1-positive fibers were $22.2 \pm 11.4\%$ at 8 weeks and $16.5 \pm 7.0\%$ at 24 weeks after injection at 10 days of age (Fig. 2E). When injected at 5 weeks of age, the mean percentages of dystrophin-positive fibers were $39.2 \pm 15.8\%$ at 8 weeks and $51.5 \pm 17.3\%$ at 24 weeks after vector injection (Fig. 2F). Next, we quantified the amount of Δ CS1 protein by immunoblotting. The amount of microdystrophin protein in the AAV-injected *mdx* muscles at 10 days of age was $12.7 \pm 8.4\%$ of that of full-length dystrophin in B10 muscle at 8 weeks (data not shown) and $9.2 \pm 1.4\%$ at 24 weeks after injection (Fig. 2G). When we injected AAV2-MCK Δ CS1 into 5-week-old *mdx* muscles, the amount was $32.6 \pm 8.0\%$ of that of B10 muscle at 8 weeks and $39.8 \pm 7.0\%$ at 24 weeks after injection (data not shown).

AAV Vector-Mediated Δ CS1 Expression Ameliorated Dystrophic Phenotypes at 24 Weeks after Injection

When we analyzed *mdx* muscles treated at 10 days of age at 24 weeks after vector injection, only a small percentage of the Δ CS1-positive fibers ($12.5 \pm 7.8\%$) had central nuclei compared with untreated *mdx* muscle fibers (Fig. 3A), suggesting the protective function of Δ CS1 against muscle degeneration. In contrast, the percentage of

FIG. 1. Diagrams of human full-length dystrophin, minidystrophin, and microdystrophin cDNAs (CS1, Δ CS1) and AAV2-MCK Δ CS1. (A) Full-length dystrophin has the N-terminal, actin-binding domain, central rod domain with 24 rod repeats and four hinges, cysteine-rich domain, and C-terminal domain. Minidystrophin, which was cloned from a mild Becker patient and reported previously, is shown as a reference [28]. CS1 has the N-terminal domain, a shortened version of the central rod domain with 4 rod repeats and three hinges, the cysteine-rich domain, and the C-terminal domain [14]. To incorporate microdystrophin CS1 cDNA into the AAV2 vector plasmid, we deleted the 3' and 5' untranslated regions and exons 71–78 from CS1 cDNA. The resultant Δ CS1 cDNA is 3.8 kb long. The number of the rod repeats or hinges is shown inside the squares. (B) Structure of the AAV2 vector expressing Δ CS1. Δ CS1 cDNA was incorporated into the AAV2 vector plasmid downstream of the truncated muscle-specific MCK promoter [15].



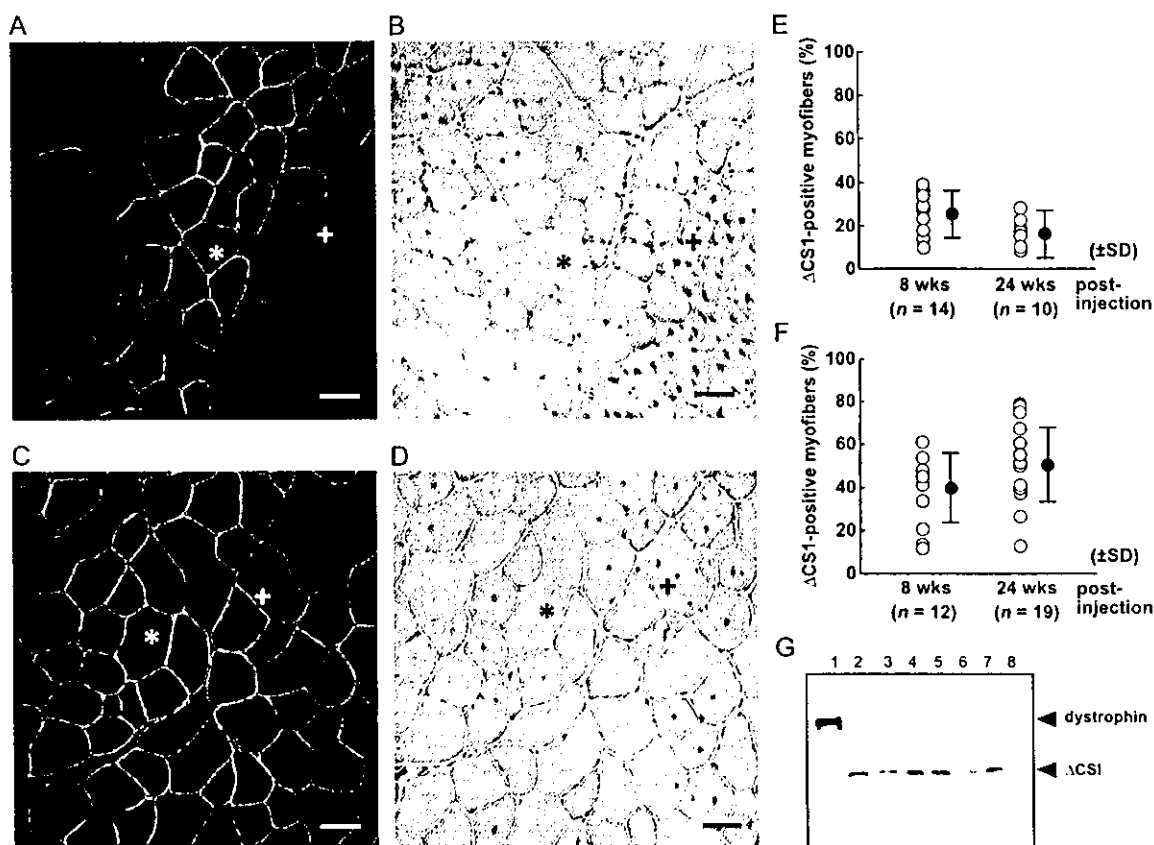


FIG. 2. Δ CS1 expression after AAV vector-mediated gene transfer into skeletal muscles of dystrophin-deficient *mdx* mice. AAV2-MCK Δ CS1 was injected into TA muscles of *mdx* mice at (A, B, E) 10 days or at (C, D, F) 5 weeks of age and the muscles were analyzed at 8 or 24 weeks after injection. (A–D) Histological analysis of AAV-injected muscles 24 weeks after AAV injection. Immunofluorescence using a dystrophin antibody (A, C) and H&E staining of serial sections (B, D) is shown. Δ CS1 is correctly localized at the sarcolemma (A, C). Most Δ CS1-positive fibers (*) showed peripherally located nuclei, and their fiber diameters were relatively larger than Δ CS1-negative fibers (+) in the muscles injected at 10 days of age (A, B). In contrast to the muscles injected at the neonatal stage, many centrally nucleated fibers (+) coexist with peripherally nucleated fibers (*) in the muscles injected with the AAV vectors at 5 weeks of age (D). In (A and C), nuclei were stained with TOTO-3 (blue). Bar, 50 μ m. (E, F) The percentage of Δ CS1-positive fibers among all fibers of the injected *mdx* muscle. The means (black circles) are indicated \pm SD (bars). The percentage of Δ CS1-positive fibers in muscles injected at 5 weeks of age (F) was higher than in the muscles injected at 10 days of age (E). (G) Western blot analysis using a dystrophin antibody of AAV-injected *mdx* muscles. Muscles treated at 10 days of age were analyzed at 24 weeks after injection. Lane 1, C57BL/10 muscle; lanes 2–7, AAV vector-injected *mdx* muscles; lane 8, uninjected *mdx* muscle. Full-length dystrophin (lane 1) and Δ CS1 (lanes 2–7) were detected at the predicted sizes (427 or 138 kDa, respectively).

centrally nucleated fibers among Δ CS1-positive fibers in *mdx* muscles treated at 5 weeks of age ($51.5 \pm 11.0\%$) was higher than that of *mdx* muscles treated at 10 days of age (Fig. 3B).

Next, we evaluated the contractile properties of AAV2-MCK Δ CS1-injected *mdx* muscle. Untreated *mdx* muscle showed remarkable hypertrophy, but its specific force was much lower than in control B10 muscle (Table 1). Similarly, the wet weight of *mdx* TA muscles treated with AAV2-MCK Δ CS1 at 10 days of age was much heavier than that of control B10 TA muscles, but importantly, the maximal force was also increased (Table 1). As a result, there was no statistical difference in specific tetanic force between AAV2-MCK Δ CS1-treated *mdx* muscles and age-matched B10 muscles (Table 1).

The transduction efficiency of AAV2 vector-mediated gene transfer into 10-day-old *mdx* mice was relatively low (only up to 20% of positive fibers) (Fig. 2E) compared to gene transfer into 5-week-old *mdx* mice (around 50%) (Fig. 2F), but, surprisingly, the specific tetanic force at 24 weeks after vector injection was almost equivalent to that of age-matched B10 mice and much higher than that of untreated *mdx* muscle (Table 1). To clarify the mechanism of force generation recovery by small percentages of Δ CS1-positive fibers, we next examined the relationship between muscle hypertrophy and force generation. We found a positive correlation ($r = 0.779$, $P < 0.05$) between the wet weight of the AAV2-MCK Δ CS1-injected TA muscle and the force generation (Fig. 4A), but not between the muscle weight and the relative interstitial

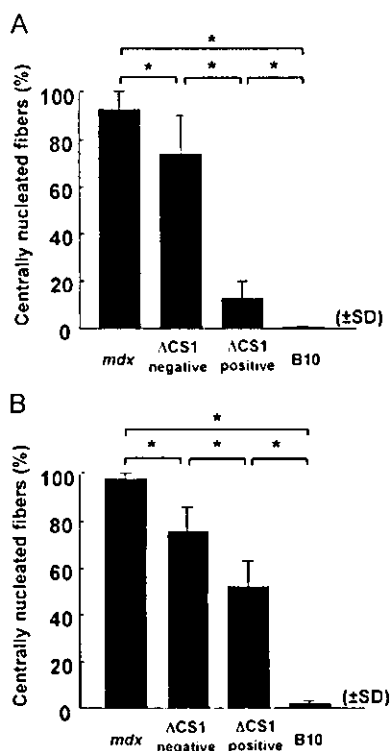


FIG. 3. Microdystrophin Δ CS1 prevents muscle degeneration. Quantitative analysis of centrally nucleated fibers among Δ CS1-positive and -negative fibers in AAV-injected *mdx* muscle. AAV2-MCK Δ CS1 was injected into TA muscles of *mdx* mice at (A) 10 days or at (B) 5 weeks of age and analyzed at 24 weeks after injection. Uninjected *mdx* and age-matched control B10 muscles were also examined. (A, B) Most of the Δ CS1-positive fibers in muscles injected at 10 days of age have peripherally located nuclei (A). The percentage of centrally nucleated fibers in Δ CS1-positive fibers in muscles treated at 5 weeks of age ($51.5 \pm 11.0\%$) (B) was higher than that in muscles treated at 10 days of age ($12.5 \pm 7.8\%$) (A). Note that the ratio of centrally nucleated fibers was significantly reduced even in Δ CS1-negative fibers in muscles injected at both ages. * $P < 0.01$.

area ($r = -0.596, P > 0.05$) (Fig. 4B). To confirm whether increased muscle weight reflected myofiber hypertrophy, we measured individual cross-sectional areas (CSAs) of Δ CS1-positive or -negative myofibers in AAV-injected *mdx* muscles. The mean value of fiber CSAs was remarkably larger in Δ CS1-positive *mdx* fibers than in B10 fibers (Fig. 4C). Histogram analysis further demonstrated that the fiber CSA distribution of Δ CS1-positive *mdx* fibers was shifted to the right compared to that of B10 muscle; larger caliber fibers were dominant, reflecting hypertrophy of Δ CS1-expressing fibers (Fig. 4E). Thus, hypertrophied Δ CS1-positive fibers seemed to greatly improve contractile force generation. Some of the untreated and Δ CS1-negative *mdx* fibers were also hypertrophied, but the hypertrophied fibers seemed not to improve the specific force (Fig. 4E).

When we injected 5-week-old mice, force generation was recovered in AAV-injected *mdx* muscles, as when

we treated 10-day-old mice, but there was no statistically significant difference in muscle weight between AAV-treated *mdx* muscles and B10 muscles (Table 1). The muscle weight had no correlation with the force generation ($r = -0.512, P > 0.05$) (data not shown). In addition, hypertrophy of Δ CS1-positive fibers was not obvious (Fig. 4D). Therefore, we concluded that improved specific force of the *mdx* muscles treated at 5 weeks of age was achieved without hypertrophy, possibly because approximately 50% of the muscle fibers were fully functional for Δ CS1 expression.

DISCUSSION

The level of dystrophin or minidystrophin expression required for effective gene therapy has not been determined yet, although estimates based on either transgenic *mdx* mouse studies [16–18] or the analysis of asymptomatic carriers of dystrophin-deficiency have been reported [19]. Clerk et al. reported that immunostaining showed very few dystrophin-negative fibers in muscles of asymptomatic DMD carriers, while immunoblot analysis revealed a considerable reduction in dystrophin [19]. Furthermore, it was reported that transgenic *mdx* mice expressing a minidystrophin at only 20–30% of endogenous dystrophin levels showed significantly reduced myopathic phenotypes [17]. Phelps et al. suggested that uniform expression of dystrophin is much more beneficial than the variable pattern when the overall levels of dystrophin expression were the same [18]. These findings suggest that the percentage of dystrophin-expressing fibers is more critical than the total amount of the protein. On the other hand, Rafael et al. showed that the expression of minidystrophin in only half the *mdx* muscle fibers resulted in a markedly milder phenotype than *mdx* mice showed [16], suggesting that dystrophin-positive fibers rescue surrounding dystrophin-negative fibers from degenerative changes. In this study, we administered a recombinant AAV vector containing a human microdystrophin gene to the *mdx* muscle and analyzed the relationship between the level or extent of microdystrophin expression and the recovery of contractile force. Importantly, relatively small percentages of muscle fibers (less than 20%) dramatically improved the specific contractile force of dystrophic muscle. Although the molecular mechanisms by which microdystrophin recovers the specific contractile force remain to be shown, this result is encouraging in that the function of dystrophin-deficient muscle might be greatly improved by fewer dystrophin-positive myofibers than previously estimated. As shown in Fig. 3, however, there is a significant reduction in the percentage of centrally nucleated fibers among Δ CS1-negative *mdx* fibers compared to untreated *mdx* muscle, suggesting that microdystrophin expression at levels below the detection limits of immunostaining might be partially protective. There-


TABLE 1: Contractile properties of AAV2-MCK Δ CS1-injected *mdx* muscle

| | Muscle length (L_0 , mm) | Muscle weight (MW, mg) | Maximal force (P_0 , mN) | Specific force ^a (mN/mm ²) |
|------------------------------|-----------------------------|------------------------|-----------------------------|---|
| Injection at 10 days of age | | | | |
| B10 ($n = 4$) | 16.1 \pm 0.9 | 48.7 \pm 2.8 | 91.3 \pm 18.1 | 32.0 \pm 5.9 |
| AAV- <i>mdx</i> ($n = 7$) | 16.1 \pm 1.2 | 64.3 \pm 4.7*** | 116.5 \pm 29.9** | 30.9 \pm 7.9** |
| <i>mdx</i> ($n = 7$) | 16.1 \pm 1.0 | 70.9 \pm 7.0* | 79.8 \pm 20.0 | 19.1 \pm 3.8* |
| Injection at 5 weeks of age | | | | |
| B10 ($n = 6$) | 15.8 \pm 0.9 | 54.9 \pm 5.7 | 69.0 \pm 31.0 | 20.9 \pm 9.0 |
| AAV- <i>mdx</i> ($n = 11$) | 15.3 \pm 0.8 | 60.9 \pm 6.8 | 81.7 \pm 24.2** | 22.3 \pm 8.2** |
| <i>mdx</i> ($n = 11$) | 15.7 \pm 0.7 | 67.9 \pm 7.6* | 42.2 \pm 26.1 | 10.9 \pm 7.5* |

Force generation was measured 24 weeks after injection. Data are expressed as means \pm SD.

^a Specific force = ($P_0 \times L_0 \times 1.06$)/MW.

* Significant difference ($P < 0.05$) compared to B10.

** Significant difference ($P < 0.05$) compared to *mdx* muscles.

fore, exact estimation of the percentage of microdystrophin-positive fibers required for the full amelioration is somewhat difficult.

Recovery of absolute maximal force and specific tetanic force is one of the barometers of amelioration. The difference between the contractile properties of Δ CS1-expressing hypertrophied muscle and those of hypertrophied *mdx* muscle by overexpression of IGF-1 [20,21] deserves attention: Δ CS1-positive *mdx* muscle showed considerable recovery of specific force, whereas IGF-mediated hypertrophy modestly restored specific force and the muscle remained susceptible to damage. Similarly, a myostatin blockade of treated *mdx* muscle reportedly improved specific force to some extent, but showed a decrease in ECC force to the same extent as control *mdx* muscle [22]. For comparison of the effects of these different approaches toward DMD therapy, the resistance of Δ CS1-treated muscle to eccentric contraction remains to be evaluated. Importantly, however, myostatin antibody-treated mice showed significantly decreased serum creatine kinase concentrations, suggesting that myostatin blockade endowed dystrophin-deficient fibers with membrane stability.

Positive correlation between muscle wet weight and specific tetanic force indicates that muscle hypertrophy is responsible for functional amelioration at 10-day-old injected *mdx* mice. However, lack of small-caliber, presumably regenerative fibers is the most prominent finding on histograms of Δ CS1-positive *mdx* muscles injected at 10 days of age. Therefore, not only a mild increase in hypertrophic fibers, but also a decrease in small-sized fibers due to inhibition of the cycle of degeneration/regeneration, could greatly contribute to normalization of specific tetanic force. Reduction in embryonic myosin heavy chain and increase in mature myosin heavy chain might contribute to the functional recovery.

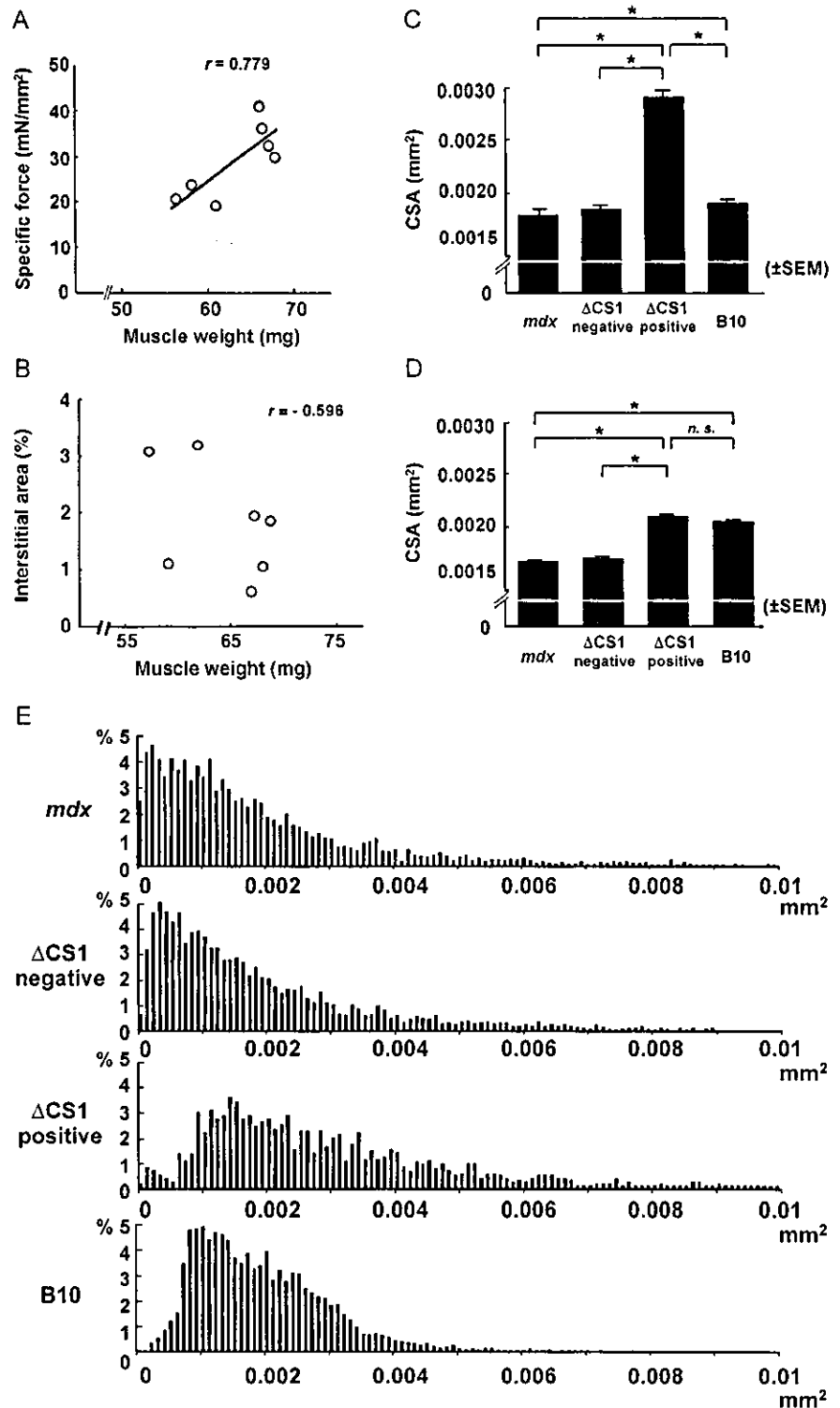
Watchko *et al.* injected an AAV2 vector carrying microdystrophin into *mdx* mice and observed incomplete

recovery of specific tetanic force with 30–60% of dystrophin-positive fibers [13]. Their microdystrophin was slightly longer than our Δ CS1, it had three hinges, and the C-terminal domain was also deleted. Subtle differences in the construction could affect the functional aspects, and therefore we think that a functional examination of transgenic *mdx* is inevitable.

We also injected AAV2-MCK Δ CS1 into 5-week-old *mdx* muscles, which usually show active cycles of muscle degeneration and regeneration. Dystrophin staining revealed that approximately 50% of *mdx* myofibers expressed human-type Δ CS1 microdystrophin 24 weeks after injection. There was no obvious sign of an immune response (data not shown). In contrast to neonatal muscle, *mdx* muscles treated at 5 weeks of age were not hypertrophied but still generated improved contractile force, indicating that widely expressed Δ CS1 could recover muscle function of adult mice without compensatory hypertrophy. Importantly, the CSAs of Δ CS1-positive fibers treated at a neonatal stage were larger than those of Δ CS1-positive fibers treated at 5 weeks of age (Figs. 4C and 4D). One possible explanation for this is that neonatal muscle has a high potency of compensatory hypertrophy in response to force deficit.

Our Δ CS1 and R4-R23/delta71-78, previously reported by Harper *et al.* [11], have similar structures. R4-R23/delta71-78 robustly transformed centrally nucleated fibers into peripherally nucleated fibers [11]. In contrast, the expression of Δ CS1 in adult *mdx* myofibers resulted in a modest reduction of centrally nucleated fibers when introduced into 5-week-old *mdx* muscle (Fig. 3B). A possible explanation for this discrepancy is a difference in the promoters that drive the microdystrophin expression. Harper *et al.* used a muscle-specific, potent promoter, CK6, and the positions of the Kozak sequences or splicing units are different from ours [11]. These differences might greatly influence the timing and levels of microdystrophin expression. A second possible factor

FIG. 4. Δ CS1-positive *mdx* fibers in AAV-treated muscle at 10 days of age show hypertrophy. TA muscles of *mdx* mice were injected with AAV2-MCK Δ CS1 at 10 days of age (A–C, E) or at 5 weeks of age (D) and analyzed at 24 weeks after injection. (A) Correlation between muscle wet weight and tetanic force generation ($n = 7$). There was a significant positive correlation between muscle weight and force generation ($r = 0.779$, $P < 0.01$). (B) Relationship between muscle weight and relative interstitial area in AAV-injected muscles ($n = 7$). The increase in muscle weight is not proportional to the interstitial area. (C, D) Mean cross-sectional area (CSA) of uninjected *mdx* muscle fibers and Δ CS1-positive or -negative fibers in AAV-injected *mdx* muscles or age-matched B10 muscle fibers. Three TA muscles were examined for each group. The total numbers of fibers traced were 9674, 6347, 1525, and 5877 in (C) and 8077, 4075, 3479, and 5476 in (D) for *mdx*, Δ CS1-negative *mdx*, Δ CS1-positive *mdx*, and B10 fibers, respectively. When injected at 10 days of age, the CSA of Δ CS1-positive *mdx* fibers was definitely larger than that of normal B10, Δ CS1-negative *mdx*, or contralateral *mdx* fibers (C). In contrast, when mice were treated at 5 weeks of age, the mean CSA of Δ CS1-positive *mdx* fibers was similar to that of B10 muscle and slightly larger than that of *mdx* or Δ CS1-negative *mdx* fibers in treated muscle (D). * $P < 0.01$. (E) Distribution of the fiber CSAs of untreated *mdx*, Δ CS1-positive, or Δ CS1-negative fibers in *mdx* muscles injected at 10 days of age and age-matched B10 fibers. Shown are the same data set presented in (C). In untreated *mdx* muscles or in Δ CS1-negative *mdx* fibers, small-caliber fibers are dominant, reflecting regeneration. The distribution pattern of Δ CS1-positive fibers deviated to the right, reflecting a larger size than that of B10 fibers. Similar to B10 muscles, small-caliber fibers were markedly reduced in Δ CS1-positive *mdx* fibers, indicating that Δ CS1 prevented muscle degeneration.



is the difference in muscle types used. Harper *et al.* injected AAV vectors into gastrocnemius muscles of 32-day-old mice. The gastrocnemius shows less centrally

nucleated fibers than TA muscle in the natural course of the disease (Yuasa *et al.*, unpublished data). In our result, however, AAV-treated *mdx* muscle with a high



percentage of centrally nucleated fibers (50%) did not show dystrophic dysfunction, e.g., decreased force generation. Therefore, centrally nucleated fibers do not disprove the protective function of Δ CS1. The percentage of centrally nucleated fibers would reflect the state of muscles at the time of injection. Our results are important because it is sometimes difficult to start gene therapies before the onset of the clinical course of DMD, and AAV2-MCK Δ CS1 is expected to show therapeutic effects even after the onset of disease.

Although we injected high titers of AAV-vector particles into the muscle, the transduction efficiency in 10-day-old *mdx* muscles was much lower than that in 5-week-old *mdx* muscle. This phenomenon was also noticed for the injection of AAV2-CMVlacZ into neonatal B10 muscle (unpublished results). This difference might be due to the preferential expression of receptors or coreceptors for an AAV-2 particle on adult muscle fibers. Several molecules, such as heparan sulfate proteoglycan [23], α V β 5 integrin [24], and dynamin I [25], are proposed to play certain roles in AAV type 2 infection, although the expression of these molecules in muscle fibers during development and aging has not been fully determined. Another possibility is dilution of AAV vectors by rapid growth of neonatal muscle. When we cultured satellite cells prepared from AAV2-CMVlacZ-injected *mdx* muscle, we observed no blue myoblasts or myotubes (data not shown). Therefore, proliferation and fusion of nontransduced satellite cells/myoblasts would greatly dilute the microdystrophin protein.

Our results are promising because AAV vector-mediated Δ CS1 gene transfer had a restorative function for dystrophin-deficient *mdx* muscle. However, demonstration of the benefits of this gene transfer strategy for human DMD patients requires careful testing. Differences between humans and mice, such as muscle size, life span, or biological properties (especially immune responses), should be taken into consideration. A bigger animal model, e.g., canine X-linked muscular dystrophy [26], will contribute to the preclinical study of gene therapy.

MATERIALS AND METHODS

Constructs of human rod-truncated microdystrophin cDNAs and generation of AAV vectors expressing microdystrophin. To incorporate microdystrophin CS1 cDNA (4.9 kb) [14] into an AAV type 2 vector, we further deleted the 3' and 5' UTRs and exons 71–78 from CS1 cDNA. In brief, DNA fragments of the 5'-terminal and 3'-terminal regions were independently amplified by PCR to remove exons 71–78 and the 5' and the 3' UTRs and then replace them with corresponding sequences of CS1 cDNA. The resulting microdystrophin cDNA was 3.8 kb long and designated Δ CS1. Microdystrophin Δ CS1 cDNA was then cloned into an AAV type 2 vector plasmid [15]. The recombinant AAV vector expressing Δ CS1 under the control of the truncated muscle-specific MCK promoter, designated AAV2-MCK Δ CS1, was then purified and titrated as previously described [15].

Administration of AAV vector to murine skeletal muscle. Fifteen microliters (7.5×10^{10} vg) or 50 μ l (2.5×10^{11} vg) of AAV2-MCK Δ CS1 was injected directly into the right TA muscles of dystrophin-deficient C57BL/10 *mdx* mice at 10 days or 5 weeks of age, respectively. AAV vector-injected and uninjected *mdx* muscles and normal muscles of age-matched C57BL/10 mice were isolated at 8 and 24 weeks after injection.

Contractile properties of AAV2-MCK Δ CS1-injected TA muscles. Tetanic force generation was measured and analyzed as described previously with some modifications [14,27]. The entire TA muscle was removed with its tibial origin intact, and the distal portion of the TA tendon and its origin was secured with a 5-0 silk suture. The TA was mounted in a vertical tissue chamber and connected to a force transducer, UL-10GR (Mineiva, Nagano, Japan), and a length servosystem, MM-3 (Narishige, Tokyo, Japan). Electrical stimulation using a SEN3301 (Nihon Kohden, Tokyo, Japan) was applied through a pair of platinum wires placed on both sides of the muscle in physiological soft solution (150 mM NaCl, 4 mM KCl, 2 mM CaCl₂, 1 mM MgCl₂, 5.6 mM glucose, 5 mM Hepes, pH 7.4, and 0.02 mM D-tubocurarine). Muscle fiber length was adjusted incrementally by using a micropositioner until peak isometric twitch force responses were obtained (optimal fiber length (L_0)). Maximal tetanic force (P_0) was assessed by stimulation frequencies of 125 pulses/s delivered in 500-ms duration trains with 2 min intervening between each train. Following two measurements, the stimulated muscle was weighed after tendon and bone attachments were removed. All forces were normalized to the physiological cross-sectional area (pCSA), the latter estimated on the basis of the following formula: muscle wet weight (in mg)/(L_0 (in mm) \times 1.06 (in mg/mm³)). The estimated pCSA was used to determine specific tetanic force (P_0 /pCSA) of the muscle. After measurement of contractile force, the muscle was quickly frozen in liquid nitrogen-cooled isopentane for histopathological analysis.

Histopathological analyses. Histological, immunohistochemical, and Western blot analyses were performed as described [14]. After blocking with an M.O.M. kit (Vector Laboratories, Burlingame, CA, USA), dystrophin was detected using a monoclonal anti-dystrophin antibody NCL-DysB (Novocastra, Newcastle, UK; 1:20 dilution) and visualized with Alexa 488-labeled goat anti-mouse IgG antibody (Molecular Probes, Eugene, OR, USA) (1:200 dilution). Nuclei were stained with TOTO-3 (Molecular Probes). In some cases, the signal was visualized with diaminobenzidine and counterstained with hematoxylin. We counted the number of centrally or peripherally nucleated fibers in dystrophin-positive or -negative fibers of whole cross sections of TA muscle. In addition, the CSA of each fiber was measured using an image analysis system, ImagePro-Plus (Media Cybernetics, Silver Spring, MD, USA). To evaluate the level of fibrosis, we performed modified Masson trichrome staining, and the blue-stained area was measured using Image Pro-Plus. The relative connective tissue area was calculated to the entire muscle cross-sectional area (%). The signals on immunoblotting were quantitated using NIH Image.

Statistical analysis. Data were expressed as means \pm SD or \pm SEM. If a significant *F* ratio was detected by analysis of variance, comparisons among each group were performed using Fisher's PLSD. A *P* value of <0.05 or <0.01 was considered statistically significant. The relation between the muscle weight and the specific tetanic force was analyzed with Pearson's correlation coefficient (*P* < 0.05).

ACKNOWLEDGMENTS

We are greatly appreciative of Ryoko Nakagawa and Satoru Mastuda for their technical support. We thank Ayako Sakamoto, Kumimasa Arima (Department of Laboratory Medicine, National Center Hospital for Mental, Nervous and Muscular Disorders), and Michiko Sagishima (Department of Pathology, School of Medicine, Teikyo University) for advising on pathological techniques. This work is supported by Grants-in-Aid from the Center of Excellence, Research on Nervous and Mental Disorders (10B-1, 13B-1), and Health Sciences Research Grants for Research on the Human Genome and Gene Therapy (H10-genome-015, H13-genome-001) from the Ministry of Health, Labor, and Welfare of

Japan, and a Grant-in-Aid for Scientific Research (B) from the Ministry of Education, Science, Sports, and Culture of Japan.

RECEIVED FOR PUBLICATION FEBRUARY 28, 2004; ACCEPTED JULY 20, 2004.

REFERENCES

1. Acsadi, G., et al. (1991). Human dystrophin expression in *mdx* mice after intramuscular injection of DNA constructs. *Nature* 29: 815–818.
2. Gilbert, R., et al. (2001). Dystrophin expression in muscle following gene transfer with a fully deleted ("guttled") adenovirus is markedly improved by trans-acting adenoviral gene products. *Hum. Gene Ther.* 20: 1741–1755.
3. DelloRusso, C., et al. (2002). Functional correction of adult *mdx* mouse muscle using gutted adenoviral vectors expressing full-length dystrophin. *Proc. Natl. Acad. Sci. USA* 99: 12979–12984.
4. Lu, Q. L., et al. (2003). Functional amounts of dystrophin produced by skipping the mutated exon in the *mdx* dystrophic mouse. *Nat. Med.* 9: 1009–1014.
5. Bartlett, R. J., et al. (2000). In vivo targeted repair of a point mutation in the canine dystrophin gene by a chimeric RNA/DNA oligonucleotide. *Nat. Biotechnol.* 18: 615–622.
6. Xiao, X., Li, J., and Samulski, R. J. (1996). Efficient long-term gene transfer into muscle tissue of immunocompetent mice by adeno-associated virus vector. *J. Virol.* 70: 8098–8108.
7. Kessler, P. D., et al. (1996). Gene delivery to skeletal muscle results in sustained expression and systemic delivery of a therapeutic protein. *Proc. Natl. Acad. Sci. USA* 26: 14082–14087.
8. Fisher, K. J., et al. (1997). Recombinant adeno-associated virus for muscle directed gene therapy. *Nat. Med.* 3: 306–312.
9. Yuasa, K., et al. (1998). Effective restoration of dystrophin-associated proteins in vivo by adenovirus-mediated transfer of truncated dystrophin cDNAs. *FEBS Lett.* 27: 329–336.
10. Wang, B., Li, J., and Xiao, X. (2000). Adeno-associated virus vector carrying human minidystrophin genes effectively ameliorates muscular dystrophy in *mdx* mouse model. *Proc. Natl. Acad. Sci. USA* 5: 13714–13719.
11. Harper, S. Q., et al. (2002). Modular flexibility of dystrophin: implications for gene therapy of Duchenne muscular dystrophy. *Nat. Med.* 8: 253–261.
12. Fabb, S. A., Wells, D. J., Serpente, P., and Dickson, G. (2002). Adeno-associated virus vector gene transfer and sarcolemmal expression of a 144 kDa micro-dystrophin effectively restores the dystrophin-associated protein complex and inhibits myofiber degeneration in nude/*mdx* mice. *Hum. Mol. Genet.* 1: 733–741.
13. Watchko, J., et al. (2002). Adeno-associated virus vector-mediated minidystrophin gene therapy improves dystrophic muscle contractile function in *mdx* mice. *Hum. Gene Ther.* 10: 1451–1460.
14. Sakamoto, M., et al. (2002). Micro-dystrophin cDNA ameliorates dystrophic phenotypes when introduced into *mdx* mice as a transgene. *Biochem. Biophys. Res. Commun.* 17: 1265–1272.
15. Yuasa, K., et al. (2002). Adeno-associated virus vector-mediated gene transfer into dystrophin-deficient skeletal muscles evokes enhanced immune response against the transgene product. *Gene Ther.* 9: 1576–1588.
16. Rafael, J., et al. (1994). Prevention of dystrophic pathology in *mdx* mice by a truncated dystrophin isoform. *Hum. Mol. Genet.* 3: 1725–1733.
17. Wells, D., et al. (1995). Expression of human full-length and minidystrophin in transgenic *mdx* mice: implications for gene therapy of Duchenne muscular dystrophy. *Hum. Mol. Genet.* 4: 1245–1250.
18. Phelps, S. F., et al. (1995). Expression of full-length and truncated dystrophin minigenes in transgenic *mdx* mice. *Hum. Mol. Genet.* 4: 1251–1258.
19. Clerk, A., et al. (1991). Characterisation of dystrophin in carriers of Duchenne muscular dystrophy. *J. Neurol. Sci.* 102: 197–205.
20. Gregorevic, P., Plant, D. R., Leeding, K. S., Bach, L. A., and Lynch, G. S. (2002). Improved contractile function of the *mdx* dystrophic mouse diaphragm muscle after insulin-like growth factor-I administration. *Am. J. Pathol.* 161: 2263–2272.
21. Barton, E. R., Morris, L., Musaro, A., Rosenthal, N., and Sweeney, H. L. (2002). Muscle-specific expression of insulin-like growth factor I counters muscle decline in *mdx* mice. *J. Cell Biol.* 157: 137–148.
22. Bogdanovich, S., et al. (2002). Functional improvement of dystrophic muscle by myostatin blockade. *Nature* 28: 418–421.
23. Summerford, C., and Samulski, R. J. (1998). Membrane-associated heparan sulfate proteoglycan is a receptor for adeno-associated virus type 2 virions. *J. Virol.* 72: 1438–1445.
24. Summerford, C., Bartlett, J. S., and Samulski, R. J. (1999). AlphaVbeta5 integrin: a co-receptor for adeno-associated virus type 2 infection. *Nat. Med.* 5: 78–82.
25. Duan, D., et al. (1999). Dynamin is required for recombinant adeno-associated virus type 2 infection. *J. Virol.* 73: 10371–10376.
26. Shimatsu, Y., et al. (2003). Canine X-linked muscular dystrophy in Japan (CXMD). *Exp. Anim.* 52: 93–97.
27. Hosaka, Y., et al. (2002). Alpha1-syntrophin-deficient skeletal muscle exhibits hypertrophy and aberrant formation of neuromuscular junctions during regeneration. *J. Cell Biol.* 16: 1097–1107.
28. England, S. B., et al. (1990). Very mild muscular dystrophy associated with the deletion of 46% of dystrophin. *Nature* 343: 180–182.



ELSEVIER

Available online at www.sciencedirect.com

SCIENCE @ DIRECT®

BBRC

Biochemical and Biophysical Research Communications 321 (2004) 1050–1061

www.elsevier.com/locate/ybbrc

Mac-1^{low} early myeloid cells in the bone marrow-derived SP fraction migrate into injured skeletal muscle and participate in muscle regeneration [☆]

Koichi Ojima ^{a,b}, Akiyoshi Uezumi ^a, Hiroyuki Miyoshi ^c, Satoru Masuda ^a,
Yohei Morita ^{d,e}, Akiko Fukase ^a, Akihito Hattori ^b, Hiromitsu Nakauchi ^{d,e},
Yuko Miyagoe-Suzuki ^a, Shin'ichi Takeda ^{a,*}

^a Department of Molecular Therapy, National Institute of Neuroscience, National Center of Neurology and Psychiatry, 4-1-1 Ogawa-higashi, Kodaira, Tokyo 187-8502, Japan

^b Department of Animal Science, Faculty of Agriculture, Hokkaido University, Kita 9, Nishi 9, Kita-ku, Sapporo, Hokkaido 060-8589, Japan

^c BioResource Center, RIKEN Tsukuba Institute, 3-1-1 Koyadai, Tsukuba, Ibaraki 305-0074, Japan

^d Laboratory of Stem Cell Therapy, Center for Experimental Medicine, The Institute of Medical Science, The University of Tokyo, 4-6-1 Shirokanedai, Minato-ku, Tokyo 108-8639, Japan

^e Department of Immunology, Institute of Basic Medical Sciences, The University of Tsukuba, and CREST (JST), 1-1-1 Tennodai, Tsukuba, Ibaraki 305-8575, Japan

Received 20 May 2004

Abstract

Recent studies have shown that bone marrow (BM) cells, including the BM side population (BM-SP) cells that enrich hematopoietic stem cells (HSCs), are incorporated into skeletal muscle during regeneration, but it is not clear how and what kinds of BM cells contribute to muscle fiber regeneration. We found that a large number of SP cells migrated from BM to muscles following injury in BM-transplanted mice. These BM-derived SP cells in regenerating muscles expressed different surface markers from those of HSCs and could not reconstitute the mouse blood system. BM-derived SP/Mac-1^{low} cells increased in number in regenerating muscles following injury. Importantly, our co-culture studies with activated satellite cells revealed that this fraction carried significant potential for myogenic differentiation. By contrast, mature inflammatory (Mac-1^{high}) cells showed negligible myogenic activities. Further, these BM-derived SP/Mac-1^{low} cells gave rise to mononucleate myocytes, indicating that their myogenesis was not caused by stochastic fusion with host myogenic cells, although they required cell-to-cell contact with myogenic cells for muscle differentiation. Taken together, our data suggest that neither HSCs nor mature inflammatory cells, but Mac-1^{low} early myeloid cells in the BM-derived SP fraction, play an important role in regenerating skeletal muscles.

© 2004 Elsevier Inc. All rights reserved.

Keywords: Side population cells; Muscle regeneration; Myogenic differentiation; Bone marrow; Muscular dystrophy

[☆] **Abbreviations:** β -Gal, β -galactosidase; BM, bone marrow; CTX, cardiotoxin; FACS, fluorescence-activated cell sorting; GC, gastrocnemius; GFP, green fluorescence protein; HE, hematoxylin and eosin; HSC, hematopoietic stem cell; MP, main population; SP, side population; TA, tibialis anterior; X-Gal, 5-bromo-4-chloro-3-indolyl β -D-galactopyranoside.

* Corresponding author. Fax: +81 42 346 1750.

E-mail address: takeda@ncnp.go.jp (S. Takeda).

Skeletal muscles have a remarkable capacity for regeneration in response to various types of damage, such as chemicals, stretching, exercise, injury, and diseases including inherited muscular dystrophies. Satellite cells are skeletal muscle-specific precursors and play an important role in muscle fiber regeneration [3]. They are located beneath the basement membrane and are mitotically

quiescent in adult muscle. Once muscle is damaged, they are activated, proliferate enormously, and fuse with each other or with pre-existing muscle fibers to produce fully mature muscle fibers [3,33]. They have been considered the only cells that give rise to myoblasts and form new myofibers in adult skeletal muscle [3,38].

Recently, cells with myogenic potential have been found in non-muscle tissues. They are involved in bone marrow (BM) [4–6,8,12,13,15,18,22,35], dorsal aorta [10], fetal liver [15], synovial membrane [11], and epidermis [24]. Among them, BM is an attractive source tissue for cell-based therapy for muscular dystrophy because it is thought that BM cells with myogenic potential are disseminated to all muscles in the body through the circulation. More recently, LaBarge and Blau [22] demonstrated that transplanted BM cells were progressively recruited as satellite cells and that subsequent exercise induced them to participate in muscle regeneration, suggesting that donor-derived BM cells contribute to muscle fibers in a step-wise biological progression.

Furthermore, it has been reported that BM side population (BM-SP) cells, which efficiently efflux Hoechst dye 33342 and enrich hematopoietic stem cells (HSCs) [16,17], participated in skeletal muscle regeneration in lethally irradiated mice [7,18]. Recently, Camargo et al. [6] and Corbel et al. [8] have reported that a single BM-SP cell was able to both reconstitute the hematopoietic system and contribute to muscle regeneration. Although Camargo et al. [6] suggested that cells committed to the myeloid lineage were incorporated into newly forming myofibers, it is still unclear what types of myeloid cells preferentially contribute to regenerating myofibers.

Several BM transplantation studies [4,6,8,12,15,18,22] indicate that donor-derived myofibers are frequently detected in regenerated fibers or in exercised muscles, although they are quite rare in normal conditions. This phenomenon is possibly related to increased recruitment of BM-derived myogenic progenitor cells or stem cells into damaged muscle via the blood stream. In addition, it is likely that cytokines released in inflamed muscles direct the myogenic commitment of BM cells.

Here we demonstrated that a large number of SP cells migrated from BM to regenerating muscles, where the BM-derived SP cells did not have hematopoietic potential but did directly participate in muscle regeneration. Further, we showed that cells with myogenic potential were enriched in BM-derived SP cells with low expression of Mac-1 antigen in regenerating muscles. These findings further support the potential of BM-SP cell-based therapy for dystrophic muscular disorders.

Materials and methods

Experimental animals. All procedures used on experimental animals were approved by the Experimental Animal Care and Use Committee

at the National Institute of Neuroscience. C57BL/6 mice were purchased from Nihon CLEA (Tokyo, Japan). C57BL/6-GFP-transgenic mice were kindly provided by Dr. Okabe (Osaka University, Japan). C57BL/6-Rosa26 mice were obtained from the Jackson Laboratory (Bar Harbor, ME).

Preparation of BM and BM-SP cells. Bone marrow cells were sterilely isolated from the femurs and tibias of GFP transgenic mice [27]. Marrow fragments were filtered through 40 μ m nitrex mesh (BD Bioscience, Franklin Lakes, NJ) and subsequently through 10 μ m nylon mesh (Kyoshin Rikoh, Tokyo, Japan). After removing red blood cells with Lympholyte-M (Cedarlane, Hornby, Ontario), BM cells were used for BM cell-transplantation or isolation of SP cells.

The BM-SP fraction was prepared as described by Goodell et al. (<http://www.bcm.tmc.edu/genetherapy/goodell/newsite/protocols.html>). BM cells were re-suspended at 10^6 cells/ml in Dulbecco's modified Eagle's medium (DMEM) (Invitrogen, Carlsbad, CA) containing 2% fetal bovine serum (FBS) (Trace Biosciences, New South Wales, Australia), 10 mM Hepes, and 5 μ g/ml Hoechst 33342 (Sigma Chemical, St. Louis, MO) and incubated for 90 min at 37°C in the presence or the absence of 50 μ M Verapamil (Sigma). For antibody staining, cells were incubated on ice for 30 min in the presence of a 1:100 dilution of PE- or APC-conjugated anti-CD45 antibody, PE-conjugated anti-CD11b/CD18 (Mac-1) antibody, PE-conjugated Sca-1 antibody, biotin-conjugated anti-CD34 antibody, or biotin-conjugated anti-c-kit antibody (BD PharMingen, San Diego, CA). For biotin-conjugated antibodies, 1:100 diluted PE- or APC-conjugated streptavidin (BD PharMingen) was further labeled for 15 min on ice. After washing, stained cells were re-suspended in PBS containing 2% FBS and 2 μ g/ml propidium iodide (PI) (BD PharMingen). Cell sorting was performed on a FACS VantageSE flow cytometer (Falcon, Franklin Lakes, NJ). Hoechst staining and subsequent antibody labeling indicated a viability of $84.2 \pm 11.5\%$ (means \pm SD, $n = 18$) as expressed by the percentage of total PI-negative cells per total cells. The BM-SP accounted for $0.026 \pm 0.017\%$ (means \pm SD, $n = 18$) of viable unfractionated BM without red blood cells. Debris and dead cells were excluded by forward scatter, side scatter, and PI gating. We used only PI-negative fractions for further experiments.

Preparation of mononucleated cells from muscle. Cardiotoxin (CTX) (Wako Pure Chemical Industries, Tokyo, Japan) -injected and uninjected skeletal muscles were dissected from GFP⁺BM-SP/CD45⁺ cell-transplanted mice and the GFP transgenic mice. We carefully removed nerves, blood vessels, tendons, and fat tissues from muscles under a dissection microscope. Trimmed muscles were minced and then treated with 0.2% type II collagenase (Worthington Biochemical, Lakewood, NJ) for 40 min at 37°C [20]. Muscle slurries were filtered through 100 μ m nitrex mesh (BD Bioscience) and subsequently through 40 μ m nitrex mesh (BD Bioscience). Erythrocytes were eliminated by treatment with 0.8% NH₄Cl in Tris-buffer solution. Mononucleated cells were stained with Hoechst 33342 and antibodies as described in BM-SP staining. Then stained cells were analyzed with a FACS VantageSE flow cytometer (Falcon). Hoechst staining and subsequent antibody labeling indicated a viability of $87.5 \pm 1.3\%$ (means \pm SD, $n = 3$) and $68.5 \pm 3.2\%$ (means \pm SD, $n = 3$) expressed as the percentage of total PI-negative cells per total mononucleated cells from injured muscles and uninjured muscles, respectively. The SP cells accounted for $0.81 \pm 0.25\%$ (means \pm SD, $n = 9$) and $1.72 \pm 0.13\%$ (means \pm SD, $n = 3$) of viable unfractionated mononucleated cells without red blood cells from injured muscles and uninjured muscles, respectively. We used only PI-negative fractions for further experiments.

Transplantation experiments. After X-irradiation with 5 or 9 Gy (Hitachi Medical, Tokyo, Japan), 5×10^6 – 1×10^7 unfractionated GFP⁺ BM cells, 2000 GFP⁺ BM-SP/CD45⁺ cells, or 3000 GFP⁺ SP/CD45⁺ cells from regenerating muscles of GFP transgenic mice were transplanted retroorbitally into 8- to 10-week-old C57BL/6 mice. For transplantation of GFP⁺ SP/CD45⁺ cells from BM and GFP⁺ SP/CD45⁺ cells from regenerating muscles, 2×10^5 unfractionated BM cells from C57BL/6 mice were also transplanted as competitor cells. SP

cells were isolated from PI-negative fractions and immediately used for transplantation assay. GFP chimerism was calculated by the ratio of GFP⁺ cells to total mononucleated cells in BM or peripheral blood. Twelve to 15 weeks after transplantation, transplanted mice were subjected to CTX injection studies and FACS analysis.

Cardiotoxin injection and tissue preparation. To induce muscle regeneration, 0.1 ml of 10 μ M CTX was injected into the TA and/or GC muscles of transplanted mice with a 27-gauge needle [9,14,19]. The CTX-injected TA and/or GC muscles and the non-injected contralateral TA and/or GC muscles were dissected for histological analysis at 3–4 weeks or 8–10 weeks after CTX injection. Following fixation with 4% paraformaldehyde in PBS for 30 min, muscles were sequentially soaked in 10% sucrose in PBS and 20% sucrose in PBS. For histological and immunohistochemical analysis, muscles were frozen in isopentane cooled with liquid nitrogen.

Histological and immunohistochemical analysis. Muscle cryostat sections (7 μ m) were stained with hematoxylin and eosin (HE). Serial cross-sections were blocked with 5% goat serum in PBS and then reacted with anti-GFP antibody (1:100; Chemicon International, Temecula, CA), anti-laminin α 2 antibody (1:100; clone 4H8-2; Alexis, San Diego, CA), anti-CD11b/18 (Mac-1) antibody (1:100; Cedarlane), and/or anti-M-cadherin antibody (1:10,000) at 4°C overnight. Anti-M-cadherin antibody was generated by fusing the mouse M-cadherin cDNA sequence corresponding to 339–444 aa to GST in a pGEX vector (Amersham Biosciences, Piscataway, NJ), and the GST-M-cadherin fusion protein was used as an antigen. The rabbit anti-serum obtained was affinity purified. The sections were incubated with appropriate combinations of Alexa 488-, Alexa 568-, and Alexa 594-labeled secondary antibodies (Molecular Probes, Eugene, OR) for 30 min. Nuclei were stained with TOTO3 (Molecular Probes). Stained sections were observed under a confocal laser scanning microscope (Leica TCS SP; Leica, Heidelberg, Germany).

Preparation of activated satellite cells. Single myofibers were prepared as described in the literature [2,31] with slight modifications. In brief, dissected extensor digitorum longus (EDL) muscles from C57BL/6 mice or C57BL/6-Rosa26 mice were digested with 0.5% type I collagenase (Worthington Biochemical) at 37°C for 90 min. Five to ten intact, viable single myofibers were plated on chamber slides (Nalge Nunc International, Naperville, IL) coated with Matrigel (Collaborative Biomedical Products, Bedford, MA), and cultured with DMEM (Invitrogen) containing 10% horse serum (HS) (BioWhittaker, Walkersville, MD) and 0.5% chick embryo extract (CEE) (Invitrogen) in a humid 5% CO₂ environment at 37°C for 4 days. To proliferate mononucleated myogenic cells, they were kept in growth medium (10% HS, 20% FBS, and 1% CEE in DMEM).

For immunostaining, cultured cells were fixed with 2% formaldehyde in PBS for 10 min. After washing with 0.5% Triton X-100 in PBS, specimens were blocked with 5% goat serum (Cedarlane) in PBS for 15 min, then incubated with anti-GFP antibody (1:500; Chemicon) and anti-sarcomeric α -actinin antibody (1:1000; Sigma) for 1 h at 37°C, and then reacted with secondary antibody conjugated with Alexa 488 or Alexa 568 (Molecular Probes). Nuclei were detected with Hoechst 33258 (Molecular Probes). To detect β -galactosidase activity, cells were stained with 5-bromo-4-chloro-3-indolyl β -D-galactopyranoside (X-Gal).

Co-culture of BM-derived SP cells with activated satellite cells. After approximately 7 days culture, myofiber-derived activated satellite cells reached 50–70% confluence. At this point, co-culture with BM-SP cells was started. Approximately 500–2500 freshly isolated GFP⁺ BM-SP/CD45⁺ cells were added to 3000–5000 activated satellite cells derived from C57BL/6 myofibers. Differentiation medium (10% HS, 2% FBS, and 0.5% CEE in DMEM) was applied soon after starting co-culture. Approximately 4000–5000 SP/CD45⁺ cells, 4000–5000 SP/CD45⁺ Mac-1⁻ cells, 2000 SP/CD45⁺ Mac-1^{low} cells, 10,000 main population (MP)/CD45⁺ cells, 10,000 MP/CD45⁺ Mac-1^{low} cells, or 10,000 MP/CD45⁺ Mac-1⁺ cells from GFP transgenic mouse muscles damaged by CTX injection were co-cultured with 10,000 activated satellite cells from C57BL/6 mice. For BM-derived SP cells from regenerating

muscles, cells were kept in growth medium (20% FBS, 2.5 ng/ml basic fibroblast growth factor (Pepro Tech EC, London, England) in DMEM) for 4 days and then switched to differentiation medium for further culture. Less than 20% of plated BM-SP cells survived 2 days after starting co-culture. Approximately 5–10% plated BM-derived cells from regenerating muscles survived 2 days after starting co-culture. Cultured cells were observed with phase-contrast and fluorescence microscopy IX70 (OLYMPUS, Tokyo, Japan).

Results

Contribution of BM-SP cells to muscle fibers in vivo

To investigate which type of donor cells contributes to muscle fibers, unfractionated BM cells or BM-SP cells from GFP transgenic mice [27] were transplanted into X-irradiated C57BL/6 mice. To further compare the efficiency of myogenic contributions of donor-derived cells to damaged muscles or intact muscles, we injected cardiotoxin (CTX) into tibialis anterior (TA) and/or gastrocnemius (GC) muscles more than 12 weeks after transplantations to induce muscle regeneration. For BM-SP cell transplantation, we selected the CD45⁺ fraction of BM-SP cells (BM-SP/CD45⁺) to exclude the possible contamination of mesenchymal stem cells [34]. The frequency of donor-derived GFP⁺ fibers in damaged muscle was relatively higher than in undamaged muscle (Fig. 1, Table 1). The ratio of GFP⁺ myofibers normalized to the number of transplanted cells was significantly higher in BM-SP/CD45⁺ cell-transplanted mice than in unfractionated BM cell-transplanted mice (Table 1). Contrary to previous reports [15,22], we have not detected donor-derived GFP⁺ satellite cells in muscle sections and in cultures of isolated single myofibers from transplanted mice (data not shown).

Migration of SP cells from BM to regenerating muscle

CTX injection experiments suggested that muscle damage enhanced the contribution of BM-SP/CD45⁺ cells to muscle fiber formation and that muscle injuries could increase the migration of BM cells with myogenic potential to the injury site via the bloodstream. Therefore, we examined whether SP cells migrate or not from BM to regenerating muscle by the use of GFP⁺ BM-SP/CD45⁺ cell-transplanted mice. Twelve to 15 weeks after transplantation, CTX was injected into TA muscles. Three days after the injury, a considerable number of donor-derived GFP⁺ cells were found in damaged muscles (Figs. 2A–D). At this early stage of muscle regeneration, M-cadherin immunostaining revealed many activated satellite cells proliferating inside the pre-existing basement membrane sheath (Fig. 2E).

Next, we isolated mononucleated cells from intact or damaged muscles and analyzed them by fluorescence-activated cell sorting (FACS). SP cells, which are sensitive to Verapamil, were involved in both intact and damaged

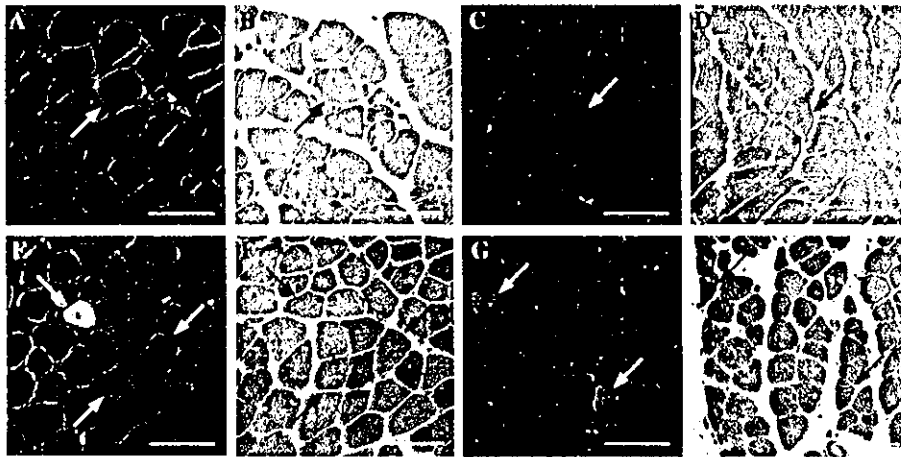


Fig. 1. Contribution of transplanted BM cells to myofibers in mice. (A–H) Unfractionated GFP⁺ BM cells (A,B,E, and F) or GFP⁺ BM-SP/CD45⁺ cells (C,D,G, and H) were transplanted into lethally X-irradiated C57BL/6 mice. Twelve to 15 weeks after transplantation, CTX was injected into TA and/or GC muscles to induce muscle regeneration (E–H). Undamaged muscles are shown in (A–D). At 10 weeks after CTX injection, cryostat sections of TA (A,B,E,F,G, and H) and GC (C,D) muscles were stained with anti-GFP antibody (green in A,C,E, and G) and anti-laminin α 2 antibody (red in A,C,E, and G). HE-stained sections (B,D,F, and H) are serial sections of (A,C,E, and G), respectively. Arrows indicate GFP-positive myofibers. Bars, 80 μ m.

Table 1
Quantitation of donor-derived myofibers in transplanted mice

| Mouse ID No. | X-ray (Gy) | Transplanted cell | GFP-chimerism in BM (%) | Muscle | CTX ^a | GFP ⁺ myofibers | Total myofibers | % ^b | % ^c |
|--------------|------------|--|-------------------------|--------|------------------|----------------------------|-----------------|----------------|----------------|
| 52 | 9 | GFP ⁺ BM | 73.4 | TA | 4w | 2 | 1368 | 0.15 | 0.0002 |
| | | | | GC | 4w | 18 | 3234 | 0.56 | 0.0018 |
| | | | | TA | — | 0 | 2120 | 0.00 | 0.0000 |
| | | | | GC | — | 4 | 3505 | 0.11 | 0.0004 |
| 4 | 5 | GFP ⁺ BM | 43.4 | TA | 8w | 5 | 1581 | 0.32 | 0.0005 |
| | | | | GC | 8w | 24 | 3093 | 0.78 | 0.0024 |
| | | | | TA | — | 2 | 1304 | 0.15 | 0.0002 |
| | | | | GC | — | 0 | 4658 | 0.00 | 0.0000 |
| 14 | 5 | GFP ⁺ BM | 46.7 | TA | 10w | 13 | 1564 | 0.83 | 0.0013 |
| | | | | GC | 10w | 44 | 1378 | 3.19 | 0.0044 |
| | | | | TA | — | 0 | 1150 | 0.00 | 0.0000 |
| | | | | GC | — | 1 | 2634 | 0.04 | 0.0001 |
| 73 | 9 | GFP ⁺ BM | 77.7 | TA | 10w | 1 | 1044 | 0.10 | 0.0002 |
| | | | | GC | 10w | 0 | 3171 | 0.00 | 0.0000 |
| | | | | TA | — | 0 | 1138 | 0.00 | 0.0000 |
| | | | | GC | — | 0 | 556 | 0.00 | 0.0000 |
| 84 | 9 | GFP ⁺ BM-SP/CD45 ⁺ | 42.7 | TA | 3w | 2 | 1205 | 0.17 | 0.1000 |
| | | | | TA | — | 0 | 1189 | 0.00 | 0.0000 |
| 106 | 9 | GFP ⁺ BM-SP/CD45 ⁺ | 22.9 | TA | 3w | 3 | 767 | 0.39 | 0.1500 |
| | | | | TA | — | 0 | 773 | 0.00 | 0.0000 |
| 61 | 9 | GFP ⁺ BM-SP/CD45 ⁺ | 92.9 | TA | 10w | 18 | 735 | 2.45 | 0.7965 |
| | | | | GC | 10w | 12 | 1176 | 1.02 | 0.5310 |
| | | | | TA | — | 0 | 584 | 0.00 | 0.0000 |
| | | | | GC | — | 4 | 2071 | 0.19 | 0.1770 |
| 69 | 9 | GFP ⁺ BM-SP/CD45 ⁺ | 10.4 | TA | 10w | 0 | 405 | 0.00 | 0.0000 |
| | | | | GC | 10w | 7 | 2838 | 0.25 | 0.3500 |
| | | | | TA | — | 0 | 1024 | 0.00 | 0.0000 |
| | | | | GC | — | 1 | 2889 | 0.03 | 0.0500 |

^a CTX was injected more than 12 weeks after transplantation. Mice were sacrificed 3, 4, 8, or 10 weeks after CTX injection.

^b % = (the number of GFP⁺ myofibers/the total number of myofibers per muscle section) \times 100.

^c % = (the number of GFP⁺ myofibers/the number of transplanted cells) \times 100.

muscles (Figs. 2F–G and I–J). To characterize SP cells in muscles, they were further fractionated by CD45 and GFP expression. GFP⁺ SP/CD45⁺ cells significantly

increased in number in injured muscles, when compared with uninjured muscles (Figs. 2H and K). In both uninjured and injured muscles, GFP⁺ SP cells were

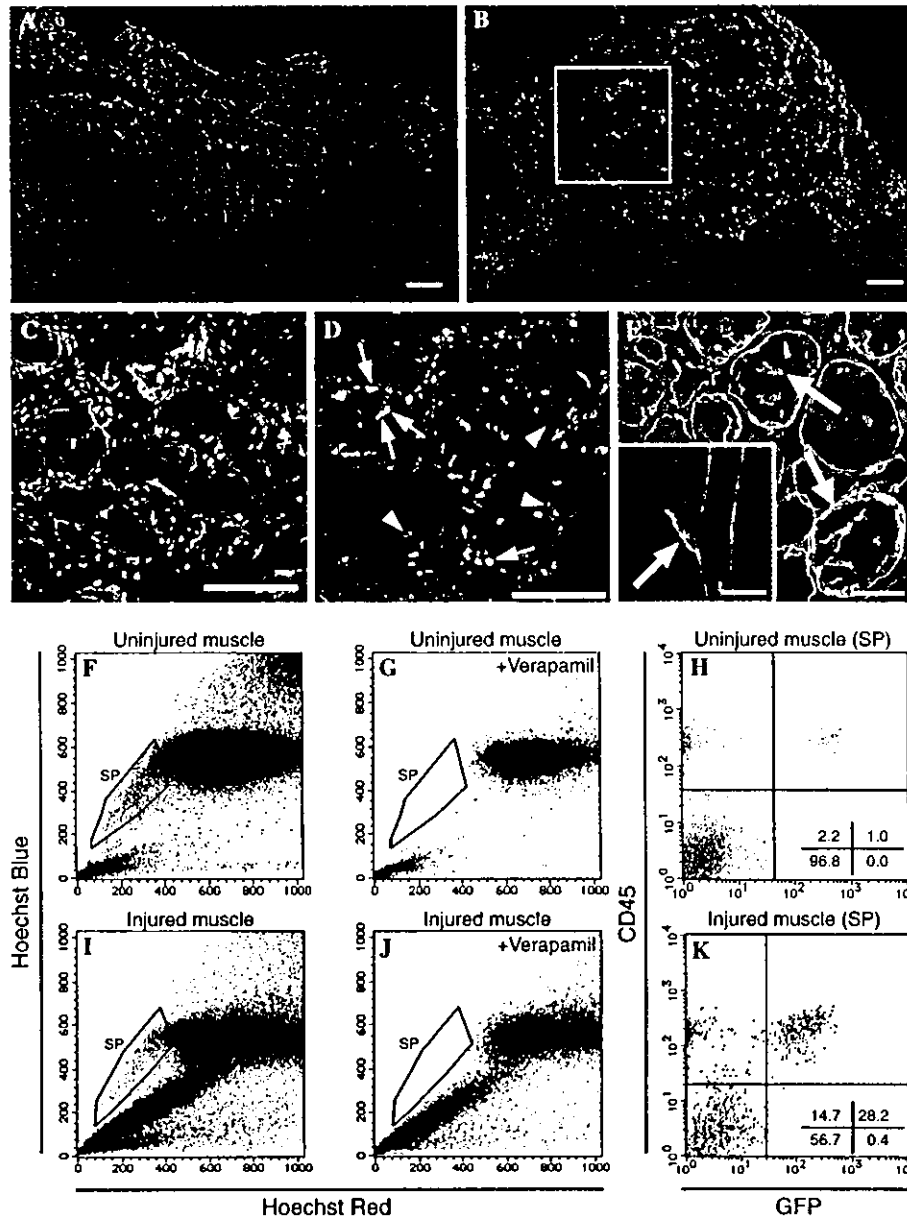


Fig. 2. Migration of BM-derived SP cells to regenerating skeletal muscle. (A,B) Immunofluorescent staining for GFP (green) and laminin $\alpha 2$ (red) of TA muscle cross-cryosections from GFP⁺ BM-SP/CD45⁺ cell-transplanted mice. (A) Only a few GFP⁺ mononucleated cells were observed in intact muscle. (B) In contrast to (A), a great number of GFP⁺ mononucleated cells have infiltrated into damaged muscle at 3 days after CTX injection. (C) A high magnification photograph of the inset area of (B), displaying triple immunofluorescent staining for GFP (green), laminin $\alpha 2$ (red), and nuclei (blue). GFP⁺ cells were located in intra- and extra-basement membranes. (D) At 3 days after CTX injection, a cryostat section of regenerating muscle of a mouse transplanted with GFP⁺ BM-SP/CD45⁺ cells was stained with anti-Mac-1 antibody (red) and anti-GFP antibody (green). Nuclei were stained with TOTO3 (blue). Arrows indicate both GFP⁺ and Mac-1⁺ positive cells. Arrowheads indicate GFP⁺ but Mac-1⁻ cells. (E) A cryostat section of regenerating muscle at day 3 after CTX injection was stained with anti-M-cadherin antibody (green) and anti-laminin $\alpha 2$ antibody (red). Nuclei were stained with TOTO3 (blue). Arrows indicate M-cadherin⁺ activated satellite cells. Our anti-M-cadherin antibody specifically recognized a satellite cell beneath the basement membrane in control muscle (arrow in inset of E). (F-K) Representative FACS analyses demonstrating that mononucleated cells isolated from uninjured muscles (F-H) or regenerating muscles (I-K) of GFP⁺ BM-SP/CD45⁺ cell-transplanted mice contained Verapamil-sensitive SP cells. These SP cells were further characterized with GFP and CD45 expression (I,K). Note that the percentage of a subfraction of SP cells expressing both GFP and CD45 was considerably increased at 3 days after CTX injection. In contrast, BM-derived SP cells expressing GFP but not CD45 were hardly detected in both regenerating and undamaged muscles. BM-GFP chimerisms of transplanted mice shown here were 93% (F-H) and 60% (I-K), respectively. Three uninjured mice and nine injured mice were analyzed and showed a similar tendency (data not shown). Bars, 100 μ m in (A-D), 40 μ m in (E), and 8 μ m in inset of (E).

largely CD45⁺ (Figs. 2I and K). Moreover, in GFP⁺ BM-transplanted mice with more than 95% chimerism, nearly 100% of GFP⁺ cells were CD45⁺ (Uezumi

et al., unpublished data), in agreement with previous reports [6,21,23]. We, therefore, selected CD45⁺ cells to pursue the fate of BM-derived cells after muscle injury.

Table 2
GFP-chimerism in peripheral blood of transplanted mice

| Number of transplanted mice | Transplanted cell ^a | Number of transplanted cells | GFP-chimerism in PB (%) ^b |
|-----------------------------|---------------------------------------|------------------------------|--------------------------------------|
| 3 | GFP ⁺ SP/CD45 ⁺ | 3000 | 0.09–0.32 |

^a Transplanted cells were prepared from CTX-injected muscles (day 3) of *GFP* transgenic mice.

^b GFP-chimerism in peripheral blood (PB) was determined at 4 weeks after transplantation.

Failure of BM-derived SP cells isolated from regenerating muscles to reconstitute the blood system of recipient mice

We observed that a large number of SP cells migrated from BM to muscles following injury. To directly examine whether migrated BM-derived SP cells in regenerating muscles had hematopoietic ability or not, we transplanted 3000 freshly isolated BM-derived SP/CD45⁺ cells from regenerating muscles of *GFP* transgenic mice into lethally irradiated recipient mice ($n = 3$). Less than 1% of the peripheral blood cells of recipient mice were donor-derived GFP⁺ blood cells 4 weeks after transplantation (Table 2), indicating that BM-derived SP cells in regenerating muscle contained very few or no hematopoietic stem and/or progenitor cells.

Analysis of surface marker expression on BM-derived SP cells

Previous studies showed that BM-SP cells and BM-derived SP cells in uninjured muscles possess hematopoietic potential [16–18,20]. However, our transplant studies suggested that BM-derived SP/CD45⁺ cells in regenerating muscles were different from HSCs even if they had the SP phenotype. To compare the surface marker expression, we isolated three different SP cells, BM-SP cells, BM-derived SP cells of uninjured muscles, and BM-derived SP cells of injured muscles. They were labeled with antibodies to CD45 and one of the following markers: Sca-1, c-kit, CD34, or Mac-1 (Fig. 3A). We detected all markers on BM-SP cells, and their expression levels were similar to previous reports [16–18,28]. We observed a small percentage of c-kit⁺ cells in the BM-derived uninjured muscle SP cells (Fig. 3A). However, importantly there were no c-kit⁺ BM-derived SP cells in injured muscles (Fig. 3A).

Interestingly, BM-derived SP cells contained Mac-1^{low} cells in both injured and uninjured muscles (Figs. 3A, C, and E). These BM-derived SP/CD45⁺ Mac-1^{low} cells in day 3 CTX-injected muscles increased in numbers (by muscle weight) approximately 18-fold, compared with uninjured muscles. We found that BM-derived SP/Mac-1^{low} cells were not labeled with anti-F4/80 antibody, which is a specific and sensitive marker for mature mouse macrophages (data not shown). In contrast, BM-derived Mac-1^{high} cells were fallen into the MP fraction (Figs. 3B–E) and expressed

F4/80 antigen (data not shown). These results suggest that SP/CD45⁺ Mac-1^{low} cells actively migrated from BM to injured muscles and that they were not mature myeloid cells.

Myogenic differentiation of BM-SP cells and BM-derived SP cells isolated from regenerating muscle

To analyze the cellular mechanism of myogenic differentiation of BM-SP cells and BM-derived SP cells from regenerating muscles in vitro, we first co-cultured BM-SP/CD45⁺ cells from *GFP* transgenic mice with activated satellite cells of C57BL/6 mice. We found that GFP⁺ BM-SP cells formed multinucleated myotubes (Fig. 4A). These myotubes expressed desmin and sometimes spontaneously contracted (data not shown). To determine whether BM-SP/CD45⁺ cells fuse with host myogenic cells or not, we co-cultured BM-SP/CD45⁺ cells prepared from *GFP* transgenic mice with activated satellite cells derived from Rosa26 mice, which express β -galactosidase (β -Gal) under a ubiquitous regulatory element [37]. X-gal staining showed that GFP⁺ myotubes expressed β -Gal, indicating that BM-SP cells fused with co-cultured host myogenic cells and formed heterokaryotic myotubes (Figs. 4B and C). When GFP⁺ BM-SP/CD45⁺ cells were cultured alone in the differentiation medium or in the conditioned medium prepared from myogenic cells, they did not form GFP⁺ myotubes (data not shown), suggesting that BM-SP/CD45⁺ cells formed myotubes via cell-to-cell contact with myogenic cells.

Next, we examined whether migrated BM-derived SP cells isolated from regenerating muscles differentiated into skeletal muscle cells in vitro or not. We focused on Mac-1 expression of BM-derived SP cells because the results, shown in Fig. 3, indicated that considerably greater number of BM-derived Mac-1^{low} SP cells infiltrated into injured muscles than into uninjured muscles. In addition, it has been recently reported that monocytes differentiate into various cell types in certain culture conditions [39]. We fractionated BM-derived cells prepared from *GFP* transgenic mouse muscles damaged by CTX injection based on both Mac-1 expression and SP phenotype: SP/CD45⁺ cells, SP/CD45⁺ Mac-1 cells, SP/CD45⁺ Mac-1^{low} cells, MP/CD45⁺ cells, MP/CD45⁺ Mac-1^{low} cells, and MP/CD45⁺ Mac-1^{high} cells. Then each fraction was co-cultured with activated satellite cells from C57BL/6 mice. After 14 days of co-culture, they were fixed and stained with anti-GFP antibody